Electronic Supporting Information (ESI) for

Enhanced electrocatalytic activity and selectivity of glycerol oxidation triggered by nanoalloyed silver-gold nanocages directly grown onto gas diffusion electrodes

Rihab Boukil,[†] Nazym Tuleushova,[†] Didier Cot,[†] Bertrand Rebiere,[‡] Valerie Bonniol,[†] Julien Cambedouzou,[†] Sophie Tingry,[†] David Cornu,[†] and Yaovi Holade[†,*]

[†]Institut Européen des Membranes, IEM UMR 5635, Univ Montpellier, ENSCM, CNRS, Montpellier, France.

[‡]Institut Charles Gerhardt Montpellier, UMR 5253, Univ Montpellier, ENSCM, CNRS, Montpellier, France

*Corresponding author (Y. H): E-mail: yaovi.holade@enscm.fr

TABLE OF CONTENTS

EXPERIMENTAL SECTION

Chemicals and Materials

GDE-based carbon paper (AvCarb MGL190, 190 μm thickness) was purchased from Fuel Cell Earth LL (USA). Ethanol (EtOH, VWR, 100%), potassium hydroxide (KOH, 99.98% (trace metal basis), Acros Organics), potassium nitrate (KNO_3, Sigma-Aldrich, 99.0% min), silver nitrate ($AgNO_3$, Premium®, 99.9995% (metals basis), Alfer aesar), trihydrate tetrachloroauric (III) acid ($HAuCl_4 \cdot 3H_2O$, 99.9%, Sigma-Aldrich), ammonia solution (30%, For analysis-ACS, Carlo Erba Reagents), sodium chloride (NaCl, ≥99.5%(AT) ACS, Sigma-Aldrich), D-(+)-glucose (99.5%, Sigma-Aldrich), potassium hexacyanoferrate ($K_3[Fe(CN)_6]$, ≥99.0%, Sigma-Aldrich), isopropanol (iPrOH, ≥99.5%, Sigma-Aldrich), Commercial catalyst is Au/C (20 wt%, ≈4 nm particles size, Premetek Co., USA) were used as-received. All used nitrogen (N_2) gas was ultrapure (Air Liquide, France) and all named ultrapure water (MQ) is provided by Milli-Q Millipore source (18.2 MΩ cm at 20 °C).

Pulse Electrodeposition of Ag onto 3D GDE: GDE@Ag

Preliminary steps. The as-received GDE electrodes were in a T-shape to yield 3 cm high, 3 cm width, and 0.19 mm thickness. Enough space on the top is reserved for further electrical wiring with gold during the electroplating. The as-cut electrodes have been washed 3× by iPrOH under middle-shacking (5 min per round) using an orbital shaker (RSLAB-7PRO, RS Lab) followed by drying in an oven at 50 °C (1 h is fine), and referred to as CP. For particles deposition onto one face of CP, an electroplating tape (3M Company) was used so that the working geometric area is 9 cm^2; however, given its 3D morphology, it is obvious that the

real geometric surface area is larger than that value. The engineered double-jacket electrochemical reactor in a three-electrode configuration has working setups of 200 mL volume (note that the full capacity is about 300 mL) and 25 °C temperature. The above CP acts as the working electrode (WE, 9 cm^2). A 22 cm^2 glassy carbon plate serves as the counter electrode (CE, Alfer aesar). A mercury-mercurous sulfate ($Hg|Hg_2SO_4|K_2SO_4$ saturated, MSE, Radiometer) acts as the reference electrode (RE). The WE-CE and WE-RE distances are about 2 and 0.5 cm, respectively.

Synthesis of GDE@Ag: Effect of the ammonia. 194 mL of 200 mM KNO_3, 6 mL of a stock solution of 5 mM $AgNO_3$ (prepared in 200 mM KNO_3) and different volumes of 0 or 15.6 µL of NH_4OH (for $R = n(NH_4OH)/n(AgNO_3) = 0, 4$) are gently stirred while outgassing for about 15 min. The switchable electroplating program (SP-150 potentiostat, Biologic Science Instruments) is composed of an OFF step (j_{appl} = 0 mA cm^{-2}, t_{OFF} = 5 s), an ON step (I_{appl} = -4.5 mA, i.e., j_{appl} = -0.5 mA cm^{-2}, t_{ON} = 5 s) and a total cycles of N_{cycles} = 126. After synthesis, the samples were thoroughly rinsed with MQ water and dried in oven at 50 °C overnight. Once dried, the scotch tape easily peeled off. The obtained free-standing catalysts are labeled as CP-Ag-R0 and CP-Ag-R4. Caution: Experiments involving the ammonia were done under a hood to prevent the release of the gaseous NH_3 directly in the Lab.

Synthesis of GDL@Ag: Effect of [$AgNO_3$]. Syntheses were performed as described above by changing the sampled volume of the stock solution of 5 mM $AgNO_3$ to yield 150 and 300 µM (filling to 200 mL working volume with NH_4OH (R = 4) and 200 mM KNO_3) and the total cycles of N_{cycles} = 126 or 252 for the two concentrations of $AgNO_3$.

Galvanic Replacement (GR) of Ag by Au at a GDE: GDE@AgAu

Typically, the above GDL@Ag electrode resulting from R = 4 and 300 μM $AgNO_3$ is equally cut into an L-shape "template sub-electrodes" of 3 cm high and 1.5 cm width (0.19 mm thickness). The working volume of the GR reactor is 15 mL, composed of 1460 μL of 5 mM $HAuCl_4$ stock solution (prepared in the filling solution) and 13.540 mL filling solution. Samples obtained using the filling solution of 0.2 M KNO_3, MQ water and 3.5 M NaCl are referred to as GR(KNO_3), GR(H_2O) and GR(NaCl), respectively. GR is performed using the aforementioned middle-shacking at room temperature (RT, about 25 ± 2 °C at that time). For the time dependent experiments, the reaction is quenched after different residence periods going from 2 min to 24 h. Once the threshold time is reached, the solution is swiftly replaced (this is done in the next 10 s) by the flushing solution, the rinsing which has been done at least 3 times by shaking the contents. Two strategies for the rinsing solution of MQ water and the above brine (3.5 M NaCl) have been considered. Once washed, the free-standing GDL@AgAu sample is dried in oven at 50 °C overnight. For the monitoring of the open circuit potential (OCP) during GR(NaCl), a tiny reference electrode (Ag/AgCl, CH Instruments, Inc.) is used, the solution is gently stirred and the potential is recorded.

Material Characterizations

Scanning electron microscope (SEM) was performed on a Hitachi S-4800 microscope. ZEISS EVOHD 15 microscope was used for energy-dispersive X-ray (EDX) analyses. To enhance the SEM/HRSEM imaging capability, a thin layer (1-5 nm) of carbon or platinum was coated on the samples. Inductively coupled plasma optical emission spectrometry (ICP-OES) analysis was performed on a spectrometer Optima 2000 DV (PerkinElmer). X-ray photoelectron spectroscopy (XPS) was fulfilled on an ESCALAB 250 spectrometer (Thermo Electron) equipped with a monochromatic radiation source Al-Kα (1486.6 eV). Survey

spectra were collected with a step of 1 eV (transition energy: 150 eV) and high-resolution spectra were recorded at a step of 0.1 eV (transition energy: 20 eV). The measurement of binding energy (BE) was corrected based on the energy of C 1s at 284.4 eV and quantifications were carried out from the corresponding XPS peak area after correction with suitable sensitivity factor. SAXS experiments were conducted in transmission geometry on a set-up involving a Mo source associated with Fox3D optics (XENOCS), delivering a monochromatic beam of wavelength = 0.71 Å. A MAR345 detector was used and the intensity was integrated around the central pixel of the detector according to a standard procedure for data treatment. After proper intensity calibration using high density polyethylene, absolute intensity was normalized to the width of the sample.

Electrochemical Measurements

Electrochemical setup and characterization. The entire electrochemical tests were fulfilled in a conventional three-electrode cell using the above potentiostat. The working electrode was a CP-based electrode cut into L-shape of 0.5 cm high and 0.5 cm width, leading to an area of 0.25 cm^2 (not taking into account the 3D structure of the GDE) and enough space on the top for electrical wiring with gold. A slab of glassy carbon plate (12.4 cm^2) was used as the counter electrode. Mercury-mercury oxide electrode (Hg|HgO|KOH 1 M, MOE, RE-61AP Reference Electrode for alkaline solution, BAS Inc.) was used as the reference electrode and was separated from the solution by a Haber-Luggin capillary tip. However, the majority of the potentials were scaled versus the reversible hydrogen electrode (RHE) according to the calibration relationship E(V vs RHE) = E(V vs MOE) + ΔE. ΔE = 0.946 V at 25 °C in 1 M KOH according to the calibrating curve reported in Fig. S2. Typically, a steady-state CV was recorded in H_2-saturated 1 M KOH at 1 mV s^{-1} by connecting a Pt plate as the working electrode, a Pt mesh as the counter electrode and that MOE as the reference electrode. The

average of the two potentials at which the current crosses zero was taken to be the thermodynamic potential for the hydrogen electrode reactions (oxidation and evolution). The catalytic ink preparation for the commercial iPrOH isopropanol and 20 µL of Nafion® suspension were ultrasonically mixed. Then, about 0.5 mg of the commercial catalyst (Au/C powder, 20 wt%, ≈4 nm particles size, Premetek Co., USA) was added. Finally, 8.4 µL of the homogeneous ink was drop-casted onto each face of a bare L-shape CP electrode of 0.5 cm height and 0.5 cm width and dried at room temperature. The estimated area of both sides is thus 0.5 cm^2 (not taking into account the 3D structure of the GDE) and enough space on the top for electrical connection with a gold wire. The Au value assessed by ICP being 19 wt.%, the loading was 16 μg_{Au} cm^{-2}. Au/C is further referred in the main text as "Vulcan-Au".

Performance towards glycerol electrocatalysis. The glycerol (0.1 M) electrooxidation reaction was investigated by the methods of cyclic voltammetry (CV) and potentiostatic electrochemical impedance spectroscopy (EIS). EIS was performed at different electrodes potentials by scanning frequencies from 100 kHz to 25 mHz (10 mV amplitude). All the voltammograms are iR-free, i.e., corrected by the "potential drop" between the working and reference electrodes according to the relationship $E_{real} = E_{applied} - R_\Omega \times I$. R_Ω is obtained by EIS at the intersection between the Nyquist curve and x-axis at high frequencies.

Electrochemical characterization by the redox probe $Fe(CN)_6^{3-}/Fe(CN)_6^{4-}$. The previous conditions were slightly modified. Since Ag or AgAu were deposited only onto 1 face, the electroplating tape (3M Company) was applied on the reaming surface to allow a rational comparison towards the redox probe $Fe(CN)_6^{3-}/Fe(CN)_6^{4-}$ that can react on both surfaces, which was not the case of glycerol. The same precaution applies for the control sample of CP. A Pt plate of 5 mm × 4 mm (both surfaces are active) was also used for comparison. The

reference electrode was a calomel saturated electrode ($Hg|Hg_2Cl_2|KCl$ saturated, SCE, SI Analytics). The experiments were performed in 0.5 M KNO_3 electrolyte in the presence of $K_3[Fe(CN)_6]$ substrate at 1 mM.

Electrolysis and high-performance liquid chromatography (HPLC). Electrolysis was fulfilled in a single compartment cell (double-jacket for the temperature control). We did not observe any change of the reaction products distribution during control experiments in an H-type cell, wherein the two compartments were separated with an anion-exchange membrane: fumapem® FAA-3-50, 45-50 μm thickness, Fuel Cell Store. The electrochemical measurements were conducted using the above potentiostat. The volume of the electrolysis was 25 mL and the temperature was fixed at 25 °C. The solution was gently stirred. The above CP@AgAu obtained by galvanic displacement in the presence of brine solution was the working electrode (cut into L-shape of 2 cm high and 1 cm width). A 22 cm^2 glassy carbon plate and Hg|HgO|KOH 1 M (MOE, RE-61AP Reference Electrode for alkaline solution, BAS Inc.) served as counter and reference electrodes, respectively. Given the 3D structure of the working electrode, we constructed a specific programmed potential electrolysis (PPE). The PPE setup consisted of two potential levels: a first potential plateau of 10 s (OFF) is fixed at E = OCP for the electrode relaxation and a second one of 10 s (ON) was set at $E = E_{ox} = 0.3$ V vs MOE (= 1.246 V vs RHE with no iR-drop correction, with iR correction, it would be ca. 0.94 vs RHE). The first plateau allows products to diffuse out of the electrode surface while the second one performed the electrooxidation of organic molecules at the surface. This program is repeated 540 times for 3 hours electrolysis experiments. The final products of glycerol electrooxidation were determined by analyzing collected samples with high-performance liquid chromatography (HPLC, Dionex ICS-1000). The injected volume is 25 μL, the column is BP-OA Benson 2000-0, which operated at room temperature. The analytes

were separated with diluted sulfuric acid (3 mmol L^{-1} H_2SO_4) used as eluent at 0.4 mL min^{-1} flow rate. The chromatograph was equipped with an UV−vis detector (λ = 210 nm). The assignments of the different peaks and the quantitative determination of the products were done with external standards, that is, by comparing the retention times with those of reference samples prepared with the expected products of glycerol electrooxidation.[3-6]

SUPPLEMENTARY TABLES

Table S1. Quantitative data from EDX of the CP-Ag material.

Entry	**CP-Ag**				
	test1	test2	test3	**average**	**SD**
	weight				
C(wt%)	51.83	43.99	47.56	47.8	3.9
O(wt%)	2.04	1.75	1.75	1.8	0.2
Ag(wt%)	46.12	54.25	50.70	50.4	4.1
atomic					
C(at%)	88.6	85.67	87.24	87.2	1.5
O(at%)	2.62	2.56	2.41	2.5	0.1
Ag(at%)	8.78	11.76	10.36	10.3	1.5

Comments: Since the carbon amount is largely underestimated (working principle of EDX that analyses only the surface), the actual silver content is highly overestimated. Indeed, it can be seen from Figs. S4 and S5 that Ag particles cover only the first three layers of microfibers of the GDE on a total of 27-21 layers.

Table S2. Quantitative data from EDX of CP-AgAu-GR(KNO_3)-10min material

Entry	**RG(KNO_3)-10min**				
	test1	test2	test3	**average**	**SD**
	weight				
C(wt%)	74.97	72.56	74.85	**74.1**	**1.4**
O(wt%)	2.55	2.98	2.64	**2.7**	**0.2**
Cl(wt%)	2.06	2.22	2.23	**2.2**	**0.1**
K(wt%)	0.00	0.00	0.00	**0.0**	**0.0**
Ag(wt%)	12.95	15.30	13.78	**14.0**	**1.2**
Au(wt%)	7.47	6.94	6.50	**7.0**	**0.5**
atomic					
C(at%)	94.33	93.41	94.13	**94.0**	**0.5**
O(at%)	2.4	2.88	2.49	**2.6**	**0.3**
Cl(at%)	0.88	0.97	0.95	**0.9**	**0.0**
K(at%)	0	0	0	**0.0**	**0.0**
Ag(at%)	1.81	2.19	1.93	**2.0**	**0.2**
Au(at%)	0.57	0.54	0.5	**0.5**	**0.0**
$Ag_{100-x}Au_x$ x =	24	20	21	**21.4**	**2.2**

Table S3. Quantitative data from EDX of CP-AgAu-GR(KNO_3)-30min material

Entry	**RG(KNO_3)-30min**					
	test1	test2	test3	test4	**average**	**SD**
	weight					
C(wt%)	54.91	53.91	55.83	56.94	**55.4**	**1.3**
O(wt%)	0.8	1.59	1.46	1.55	**1.4**	**0.4**
Cl(wt%)	6.5	6.60	6.70	6.28	**6.5**	**0.2**
K(wt%)	0.09	0.17	0.00	0.00	**0.1**	**0.1**
Ag(wt%)	26.16	26.05	25.30	24.44	**25.5**	**0.8**
Au(wt%)	11.34	11.42	10.71	10.78	**11.1**	**0.4**
atomic						
C(at%)	89.42	88.2	89.09	89.51	**89.1**	**0.6**
O(at%)	0.98	1.96	1.75	1.83	**1.6**	**0.4**
Cl(at%)	3.59	3.66	3.62	3.35	**3.6**	**0.1**
K(at%)	0.05	0.09	0	0	**0.0**	**0.0**
Ag(at%)	4.74	4.74	4.5	4.28	**4.6**	**0.2**
Au(at%)	1.14	1.14	1.04	1.03	**1.1**	**0.1**
$Ag_{100-x}Aux$ x =	19	19	19	19	**19.2**	**0.3**

Table S4. Quantitative data from EDX of CP-AgAu-GR(H_2O)-10 min material

Entry	**RG(H_2O)-10min**				
	test1	test2	test3	**average**	**SD**
	weight				
C(wt%)	72.44	72.87	71.28	**72.2**	**0.8**
O(wt%)	1.47	1.95	1.55	**1.7**	**0.3**
Cl(wt%)	2.49	3.05	3.30	**2.9**	**0.4**
Ag(wt%)	14.83	16.53	17.02	**16.1**	**1.1**
Au(wt%)	8.77	5.60	6.87	**7.1**	**1.6**
atomic					
C(at%)	94.6	93.97	93.95	**94.2**	**0.4**
O(at%)	1.44	1.89	1.53	**1.6**	**0.2**
Cl(at%)	1.1	1.33	1.47	**1.3**	**0.2**
Ag(at%)	2.16	2.37	2.5	**2.3**	**0.2**
Au(at%)	0.7	0.44	0.55	**0.6**	**0.1**
$Ag_{100-x}Au_x$ x =	24	16	18	**19.4**	**4.6**

Table S5. Quantitative data from EDX of CP-AgAu-GR(H_2O)-5min material

Entry	**RG(H_2O)-5min**				
	test1	test2	test3	**average**	**SD**
	weight				
C(wt%)	63.89	55.27	63.48	**60.9**	**4.9**
O(wt%)	1.62	1.42	1.87	**1.6**	**0.2**
Cl(wt%)	5.42	6.51	5.32	**5.8**	**0.7**
Ag(wt%)	20.57	23.67	19.01	**21.1**	**2.4**
Au(wt%)	8.49	13.13	10.31	**10.6**	**2.3**
atomic					
C(at%)	91.59	89.18	91.43	**90.7**	**1.3**
O(at%)	1.75	1.71	2.02	**1.8**	**0.2**
Cl(at%)	2.63	3.56	2.6	**2.9**	**0.5**
Ag(at%)	3.28	4.25	3.05	**3.5**	**0.6**
Au(at%)	0.74	1.29	0.91	**1.0**	**0.3**
$Ag_{100-x}Au_x$ x =	18	23	23	**21.6**	**2.7**

Table S6. Comparative performance of relevant glycerol electrooxidation reaction on metallic catalysts in alkaline media from literature.

The metal loading is normalized to the geometric area. WE: working electrode. C: carbon black Vulcan. *L*: metal loading on the electrode, per square centimeter of the electrode. Glyc.: glycerol *T*°: temperature. RT: room temperature. E_{onset}: onset potential. j_p: peak current density and expressed in either amps per milligram of metal (A mg^{-1}) or milliamps per square centimeter of the electrode (mA cm^{-2}). ACF: activated carbon felt electrode. GDE: gas diffusion electrode. CP: carbon paper. Empty box (–) means that the original article does not provide the data.

Ref.	Electrode material			Conditions		Performance (50 mV s^{-1} at scan rate)		
	Nanocatalyst (metal loading)	WE (area)	*L* (μg cm^{-2})	Electrolyte + Glyc.	T° (°C)	E_{onset} (V vs RHE)	j_P (A mg^{-1})	j_P (mA cm^{-2})
Herein	GDE@(0.17 wt.%): 0.25 cm^2		16	1 M KOH + 0.1 Glyc.	25	0.3	18.2	290
	Au/C (20 wt.%)	CP (0.25 cm^2)	16	1 M KOH + 0.1 Glyc	25	0.70	2.8	44
Adv. Mater., 2019, 31, 1804763.[7]	Pt in N-doped graphene nanomesh on carbon cloth	GC (0.07 cm^2)	300	1 M KOH + 0.1 Glyc	–	0.28	2.9	–
Energy Environ. Sci., 2016, 9, 3097-3102.[8]	Pd/C nanosponge	GC (0.07 cm^2)	–	1 M KOH + 0.1 Glyc.	–	0.65	–	15

Energy Environ. Sci., 2015, 8, 2910-2915.[9]	Pd nanowire networks	GC (–)	25.5	1 M KOH + 0.1 Glyc.	–	0.60	0.6	–
Appl. Catal. B: Env., 2019, 245, 604-612.[10]	Pt_4Au_6@Ag	GC (0.07 cm^2)	500	0.1 M KOH + 1 Glyc.	RT	0.50	–	3.1
ACS Appl. Mater. Interfaces., 2019, 11, 28953-28959.[11]	PtAg	GC (0.07 cm^2)	–	0.1 M KOH + 1 M Glyc.	–	0.50	–	7.57
J. Mater. Chem. A, 2018, 6, 24418-24424[12]	Pt_3Co_1 nanowires	GC (0.07 cm^2)	–	1 M KOH +1 M Glyc.	–	0.4	3.8	7.2
Nanoscale, 2017, 9, 12996-13003.[13]	Au_1Ag_1 (core/shell nanospheres)	GC (0.07 cm^2)	28.5	1 M KOH +1 M Glyc.	RT	0.97	3.5	–

J. Am. Chem. Soc., 2014, 136, 3937-3945.[14]	Pd sel-supported	GC (0.25 cm^2)	200	1 M KOH + 0.1 Glyc.	–	0.6	0.1	–
RSC Adv., 2014, 4, 64476-64483.[15]	Pd/C (40 wt.%)	GC (0.07 cm^2)	320	0.1 M KOH + 0.1 Glyc.	–	0.65	0.025	–
ACS Catal., 2013, 3, 2403-2411.[3]	Pd/C (30 wt.%)	GC (0.07 cm^2)	116	0.1 M NaOH + 0.1 Glyc.	RT	0.50	0.16	–
Appl. Catal. B: Env., 2010, 93, 354-362.[16]	Pd/C (40 wt.%)	GC (0.07 cm^2)	142	1 M KOH + 0.1 Glyc.	20	0.6	–	25
ChemElectroChem, 2016, 3, 1694-1704.[17]	$Pt_3Pd_6Bi_1$/C (40 wt.%)	GC (0.07 cm^2)	100	1 M NaOH + 0.1 Glyc.	RT	0.4	–	40
ChemElectroChem, 2017, 4, 39-45.[18]	$Pt_{86}Ru_{14}$/C (40 wt.%)	GC (0.07 cm^2)	320	1 M NaOH + 1 Glyc.	RT	0.5	0.6	–

Electrochem. Commun., 2013, 34, 185-188.[19]	Pd	GC (0.07 cm^2)	200	1 M NaOH + 0.1 Glyc.	RT	0.63	0.4	–
Chem. Commun., 2017, 53, 1642-1645.[20]	Pd nanosheets	GC (0.07 cm^2)	137	1 M NaOH + 0.1 Glyc.	RT	0.50	0.55	70
ChemElectroChem, 2018, 5, 743-747.[21]	ACF@Pd (1 wt.%): ~1 cm^2		96	0.1 M KOH + 0.1 Glyc.	RT	<0.5	0.44	40

Table S7. Fitted EIS data from the used equivalent electrical circuit (R_Ω+Q_{CPE}//R_{ct}).

The electrode surface is 0.25 cm^2. Electrode = "CP-AgAu-GR(NaCl)-5min"

E_{appl}(V vs RHE)	ohmic resistance $R_\Omega(\Omega)$	charge transfer resistance $R_{ct}(\Omega)$	constant phase element	
			$Q_{CPE}(\mu F\ s^{(a-1)})$	a
0.75	3.3	189.8	395	0.88
0.80	3.3	145.5	350	0.89
0.85	3.3	74.2	305	0.91
0.90	3.3	31.3	293	0.92
0.94	3.3	16.0	299	0.92
1.00	3.3	8.2	290	0.93

Table S8. Fitted EIS data from the used equivalent electrical circuit (R_Ω+Q_{CPE}//R_{ct}).

The electrode surface is 0.25 cm^2. Electrode = "CP-Au". Working electrode area = 0.25 cm^2

E_{appl}(V vs RHE)	ohmic resistance $R_\Omega(\Omega)$	charge transfer resistance $R_{ct}(\Omega)$	constant phase element	
			$Q_{CPE}(\mu F\ s^{(a-1)})$	a
0.75	3.4	240.7	93.0	0.93
0.80	3.4	161.2	89.4	0.93
0.85	3.4	107.1	87.6	0.93
0.94	3.4	15.5	100.0	0.91
1.00	3.4	7.5	133.0	0.87

Table S9. Fitted EIS data from the used equivalent electrical circuit (R_Ω+Q_{CPE}//R_{ct}).
The electrode surface is 0.5 cm^2. Electrode = "Vulcan-Au"

E_{appl}(V vs RHE)	ohmic resistance $R_\Omega(\Omega)$	charge transfer resistance $R_{ct}(\Omega)$	constant phase element	
			$Q_{CPE}(\mu F\ s^{(a-1)})$	a
0.75	3.8	149.5	484.5	0.91
0.80	3.9	78.8	480.5	0.90
0.85	3.9	36.8	516.9	0.89
0.90	3.8	17.9	570.0	0.87
0.94	3.8	10.9	694.2	0.84
1.00	3.8	9.9	1002.0	0.80

Table S10. Electrochemical kinetics data from the electrodes surface probing using the redox couple $Fe(CN)_6^{3-}/Fe(CN)_6^{4-}$.
The modeling curve of Figure S19 is used. iR-free CVs were recorded at 100 mV s^{-1} in 0.5 M KNO_3 + 1 mM $K_3[Fe(CN)_6]$ at 25 °C. Error bars represent 1 SD (*n* = 3). For CP-AgAu, the galvanic replacement (GR) was performed in a brine solution.

Entry	ΔE_p(mV)	$k°(10^{-3}$ cm $s^{-1})$	$R_{ct}(\Omega\ cm^2)$	$j_0(10^{-3}$ A $cm^{-2})$
CP	458.2±2.1	0.26±0.01	1006.6±6.2	25.5±0.2
CP-Ag	241.6±1.9	0.69±0.01	383.9±5.1	66.9±0.9
CP-AgAu	139.7±6.6	1.98±0.20	135.4±14.3	191.1±19.4
Pt bulk	76.5±2.1	12.61±1.84	21.4±2.9	1216.5±177.2

Table S11. Fitted EIS data from the used equivalent electrical circuit "$R_{\Omega}+Q_{CPE}//(R_{ct}+W)$". Experiments were performed 0.5 M KNO_3 + 1 mM $K_3[Fe(CN)_6]$ at 25 °C at E_{appl}(= OCP) = 0.25 ± 0.01 V vs SCE. For CP-AgAu, the galvanic replacement (GR) was performed in a brine solution.

Entry	$R_W(\Omega\ cm^2)$	$R_{ct}(\Omega\ cm^2)$	$Q_{CPE}(\mu F\ cm^2\ s^{(a-1)})$	a	$W(\Omega\ cm^2\ s^{-1/2})$
CP	3.1	1843.8	1.1	0.90	1103.8
CP-Ag	2.9	626.8	2.0	0.90	525.0
CP-AgAu	2.9	170.5	4.3	0.87	279.3
Pt bulk	4.3	38.4	7.2	0.90	508.8

Table S12. Quantitative data from EDX of CP-AgAu-GR(H_2O)-washed(NaCl)-5min material

Entry	**GR(H_2O)-washed(NaCl)-5min**				
	test1	test2	test3	**average**	**SD**
	weight				
C(wt%)	87.17	80.12	86.62	**84.6**	**3.9**
O(wt%)	2.50	2.04	2.29	**2.3**	**0.2**
Cl(wt%)	0.06	0.22	0.09	**0.1**	**0.1**
Ag(wt%)	0.44	0.79	0.41	**0.5**	**0.2**
Au(wt%)	9.83	16.83	10.59	**12.4**	**3.8**
atomic					
C(at%)	97.16	96.72	97.23	**97.04**	**0.28**
O(at%)	2.09	1.85	1.93	**1.96**	**0.12**
Cl(at%)	0.02	0.09	0.04	**0.05**	**0.04**
Ag(at%)	0.05	0.11	0.05	**0.07**	**0.03**
Au(at%)	0.67	1.24	0.75	**0.89**	**0.31**
$Ag_{100-x}Au_x$ x =	93	92	94	**93**	**1**

Table S13. Quantitative data from EDX of CP-AgAu-GR(NaCl)-5min material

Entry	RG(NaCl)-5min					
	test1	test2	test3	test4	**average**	**SD**
	weight					
Cl(wt%)	0	0	0	0	**0**	**-**
Ag(wt%)	7.04	7.20	7.45	7.97	**7.42**	**0.41**
Au(wt%)	92.96	92.80	92.55	92.03	**92.59**	**0.41**
atomic						
Cl(at%)	0	0	0	0	**0**	**-**
Ag(at%)	12.15	12.40	12.81	13.65	**12.75**	**0.66**
Au(at%)	87.85	87.60	87.19	86.35	**87.25**	**0.66**
$Ag_{100-x}Au_x$ x =	88	88	87	86	**87**	**1**

Table S14. Quantitative data from the electrolysis and HPLC of GDE@AgAu material.

Retention time (min)	HPLC			
	Name	stoichiometric coefficient ν	Concentration C(mM)	Selectivity (%)
11.45	Oxalic acid	1.5	2.2	1.8
11.65	Mesoxalic acid	1.0	0.0	0.0
12.76	Tartronic acid	1.0	0.2	0.1
17.66	Glyceric acid	1.0	1.3	0.7
20.02	Glycolic acid	1.5	40.0	31.9
22.31	formic acid	3.0	41.0	65.5

$$\nu = \frac{number\ of\ \ carbon\ atoms\ in\ the\ \ glycerol}{number\ of\ \ carbon\ atoms\ in\ the\ \ product}$$

$$Selectivity = 100 \times \frac{\nu_i C_i}{\sum_{i=1}^{i=3} \nu_i C_i}$$

where *i* is the compound.

Table S15. Post-mortem quantitative data from EDX of CP-AgAu-GR(NaCl)-5min material after 3 h of bulk electrolysis.

$E_{applied}$ = 0.3 V vs MOE = 1.246 V vs RHE with no iR-drop correction. Temperature = 25 °C.

Entry	RG(NaCl)-5min_Electrolysis_3h							
	test1	test2	test3	test4	test5	test6	**average**	**SD**
	weight							
Ag(wt%)	11.26	11.04	9.65	10.49	12.07	10.60	**10.85**	**0.82**
Au(wt%)	88.74	88.96	90.35	89.51	87.93	89.40	**89.15**	**0.82**
atomic								
Ag(at%)	18.81	18.48	16.32	17.63	20.04	17.80	**18.18**	**1.25**
Au(at%)	81.19	81.52	83.68	82.37	79.96	82.20	**81.82**	**1.25**
$Ag_{100-x}Au_x$ x =	81	82	84	82	80	82	**82**	**1**

SUPPLEMENTARY FIGURES

Method for Ag Nanostructured Particles Growth at GDE.

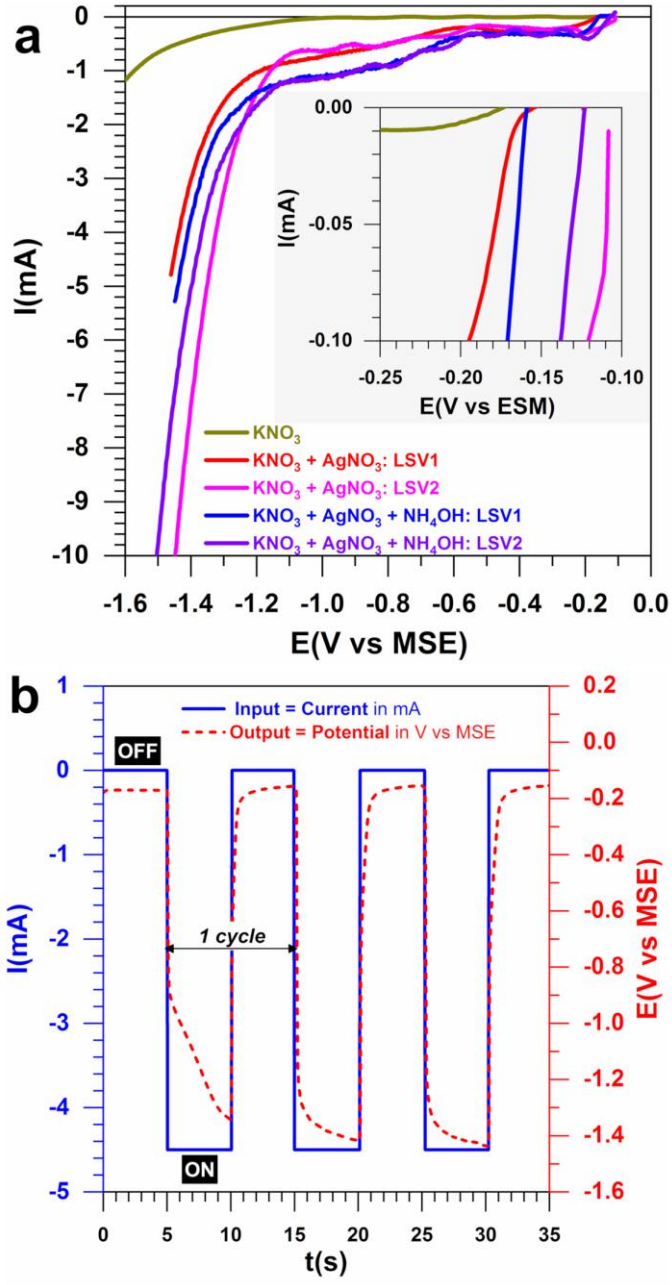

Fig. S1. The developed method for the direct growth of Ag NPs onto the surface of GDE.

(a) Control LSV curves obtained at 5 mV s^{-1} in MQ water in the presence of different chemical species: 200 mM KNO_3, 0.15 mM $AgNO_3$, and 0.60 mM NH_4OH (R = 4). (b) Program of the pulse electrodeposition at a GDE: The applied current (input, left *y*-axis) and the response of the potential (output, right *y*-axis) as a function of time during the first cycles. The temperature is 25 °C.

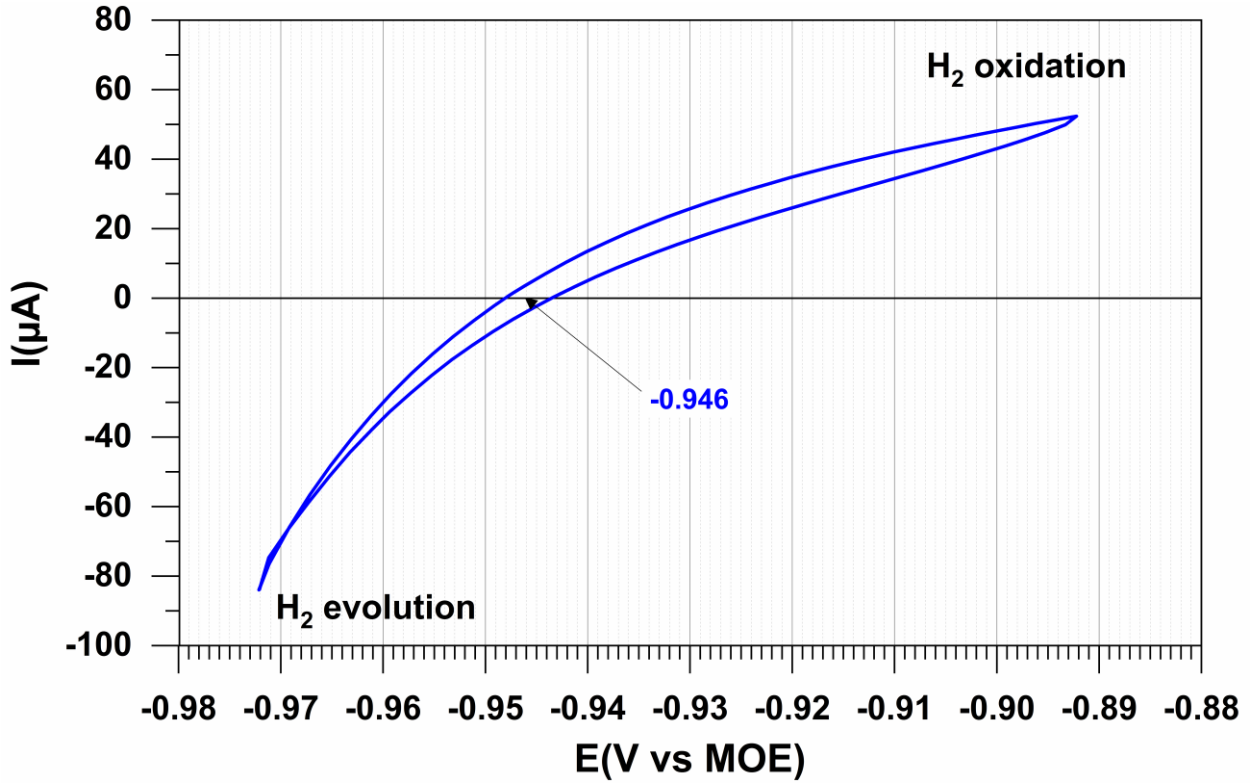

Fig. S2. CV for the calibration of the reference electrode.

Steady-state CV recorded in H_2-saturated 1 M KOH at 1 mV s^{-1} at 25 °C by employing a Pt plate as the working electrode, a Pt mesh as the counter electrode and a Hg|HgO|KOH 1 M as the reference electrode, referred to as MOE. Note: NB: experiments were performed in a quiescent solution.

Results: The average of the two potentials at which the current crossed zero is taken to be the thermodynamic potential for the hydrogen electrode reactions. Thus, the scaling relationship is as following:

$$E(\text{V vs RHE}) = E(\text{V vs MOE}) + 0.946$$

Characterization of the used GDE

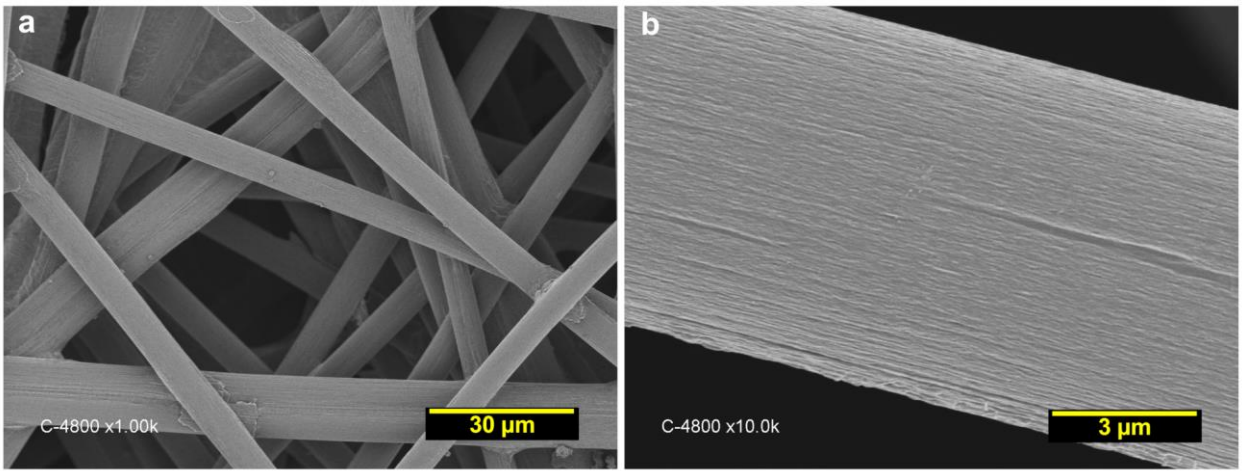

Fig. S3. SEM/HRSEM pictures of the used GDE-based carbon paper (AvCarb MGL190, 190 µm thickness).
(a) SEM image and (b) HRSEM micrograph.

The white color results from the deposition of a thin layer (1-5 nm) of Pt to enhance the imaging capability. The SEM images show different fibers (filled tubes) with a diameter of 7-9 µm. Since the thickness is 190 µm, it can be deduced that the entire 3D network is composed of ca. 27-21 layers of microfibers.

Optimization for Metal Particles Growth on the Surface of GDE.

Effect of Ag^+ Complexation by NH_3 on the Ag Particles Growth onto GDE

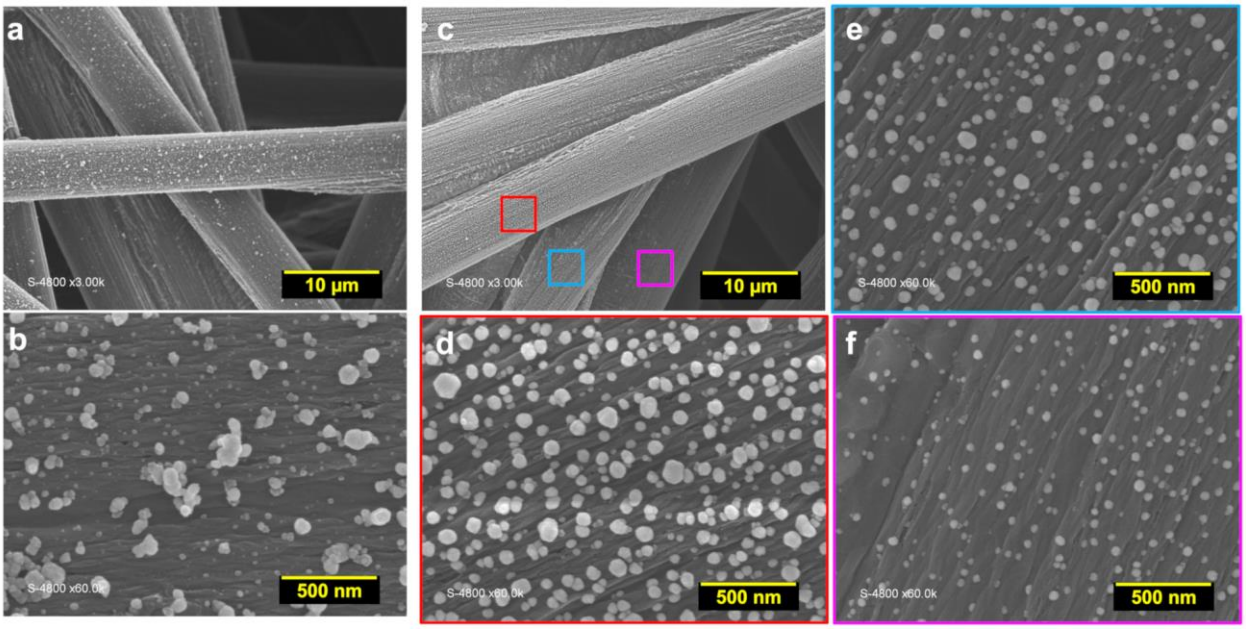

Fig. S4. SEM micrographs of Ag grown onto a GDE for different ratios R = n(NH_4OH)/n($AgNO_3$).
Conditions of 200 mM KNO_3, 0.15 mM $AgNO_3$, 0.60 mM NH_4OH, j_{appl} = -0.5 mA cm^{-2}; t_{OFF} = t_{ON} = 5 s; N_{cycles} = 126 and temperature = 25 °C. (a, b) R = 0; (c-f) R = 4.

Results: Upon the introduction of ammonia in the reactor containing aqueous solution of $AgNO_3$, the chemical equilibrium and electrochemical reduction reactions are described below. The strong decrease of the standard redox potential of Ag(I) from 0.80 to 0.37 V vs SHE enables lowering the reduction kinetics, which leads to a tight control of the seed growth into homogeneous particles (Figure S4b versus Figure S4d).

$$NH_4OH + H_2O \rightarrow NH_3 + OH^- \qquad pK_a = 9.2$$

$$Ag^+ + 2NH_3 \rightarrow Ag^+(NH_3)_2 \qquad K_f = \frac{1}{K_d} = 10^{7.2}$$

$$Ag^+ + e^- \rightarrow Ag \qquad E° = 0.8 \text{ V vs SHE}$$

$$Ag^+(NH_3)_2 + e^- \rightarrow Ag + 2NH_3 \qquad E°' = E° - \frac{2.3RT}{nF} pK_d = 0.37 \text{ V vs SHE}$$

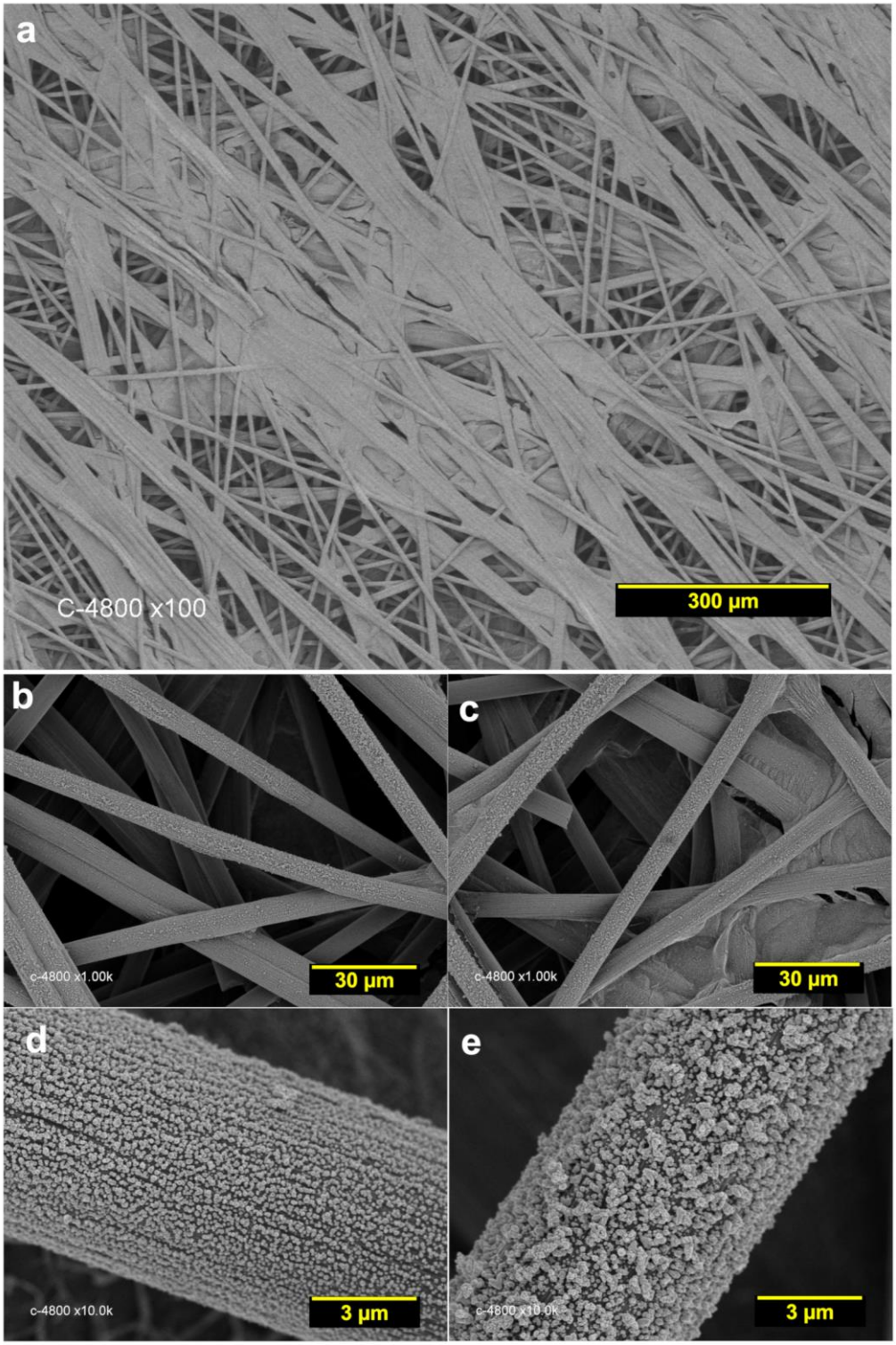

Fig. S5. Overview SEM micrographs of Ag grown onto a GDE for the ratio R = $n(NH_4OH)/n(AgNO_3)$ = 4

(a-e) Images at different magnifications. Synthesis conditions: 200 mM KNO_3, 0.30 mM $AgNO_3$, 1.20 mM NH_4OH, j_{appl} = -0.5 mA cm^{-2}; t_{OFF} = t_{ON} = 5 s; N_{cycles} = 252 and temperature = 25 °C.

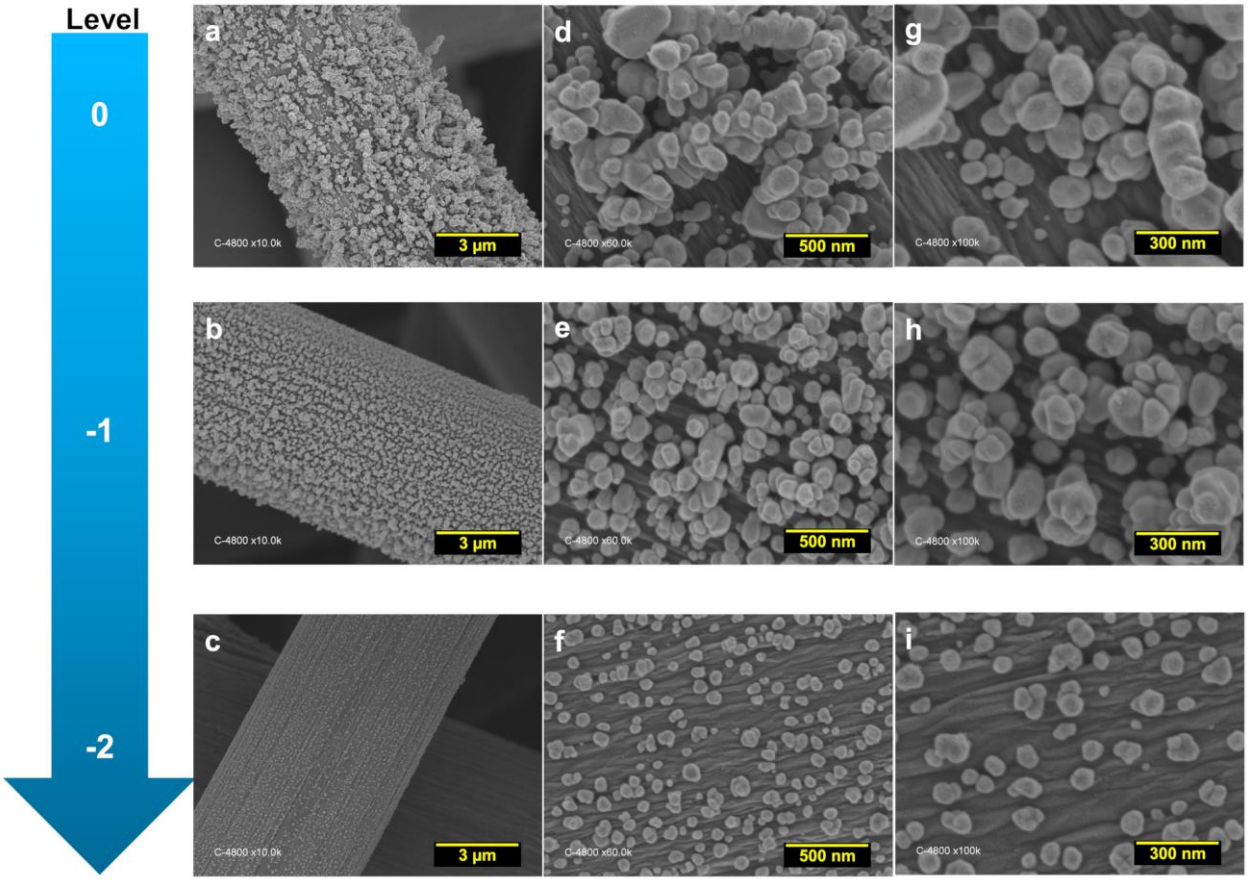

Fig. S6. SEM/HRSEM micrographs of Ag grown onto a GDE for the ratio R = n(NH_4OH)/n($AgNO_3$) = 4 to illustrate the deposition within the 3D structure of GDE.
(a-i) Images at different magnifications. Synthesis conditions: 200 mM KNO_3, 0.30 mM $AgNO_3$, 1.20 mM NH_4OH, j_{appl} = -0.5 mA cm^{-2}; t_{OFF} = t_{ON} = 5 s; N_{cycles} = 252 and temperature = 25 °C. The arrow indicates the level of the fiber starting from: (a, d, g) first or surface (top), (b, e, h) second and (c, f, i) third.

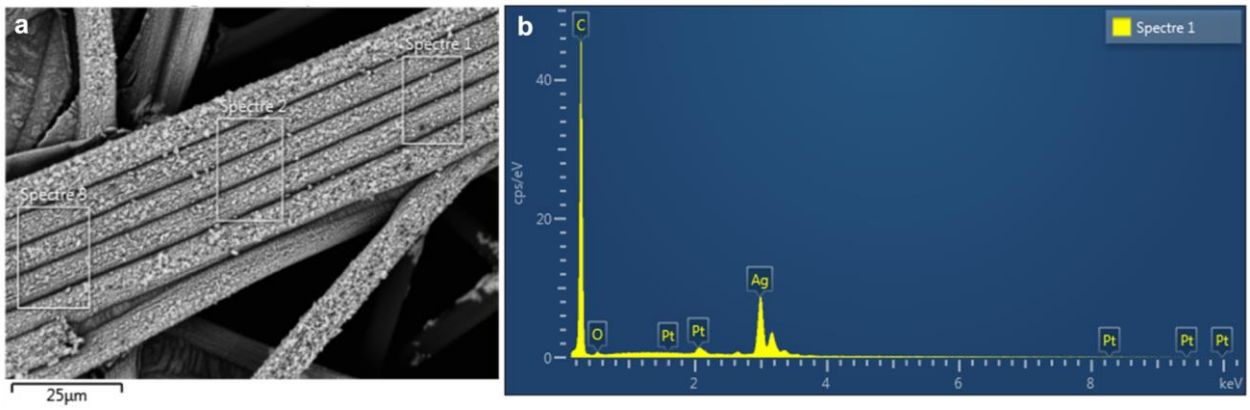

Fig. S7. EDX analysis of Ag grown onto a GDE for the ratio R = n(NH_4OH)/n($AgNO_3$) = 4 (a) Overview SEM micrograph and (b) EDX profile. Synthesis conditions: 200 mM KNO_3, 0.30 mM $AgNO_3$, 1.20 mM NH_4OH, j_{appl} = -0.5 mA cm^{-2}; t_{OFF} = t_{ON} = 5 s; N_{cycles} = 252 and temperature = 25 °C. Please: Read “Spectre” as “Spectra”. NB: the signal of Pt comes from the sample preparation to enhance the SEM imaging capability.

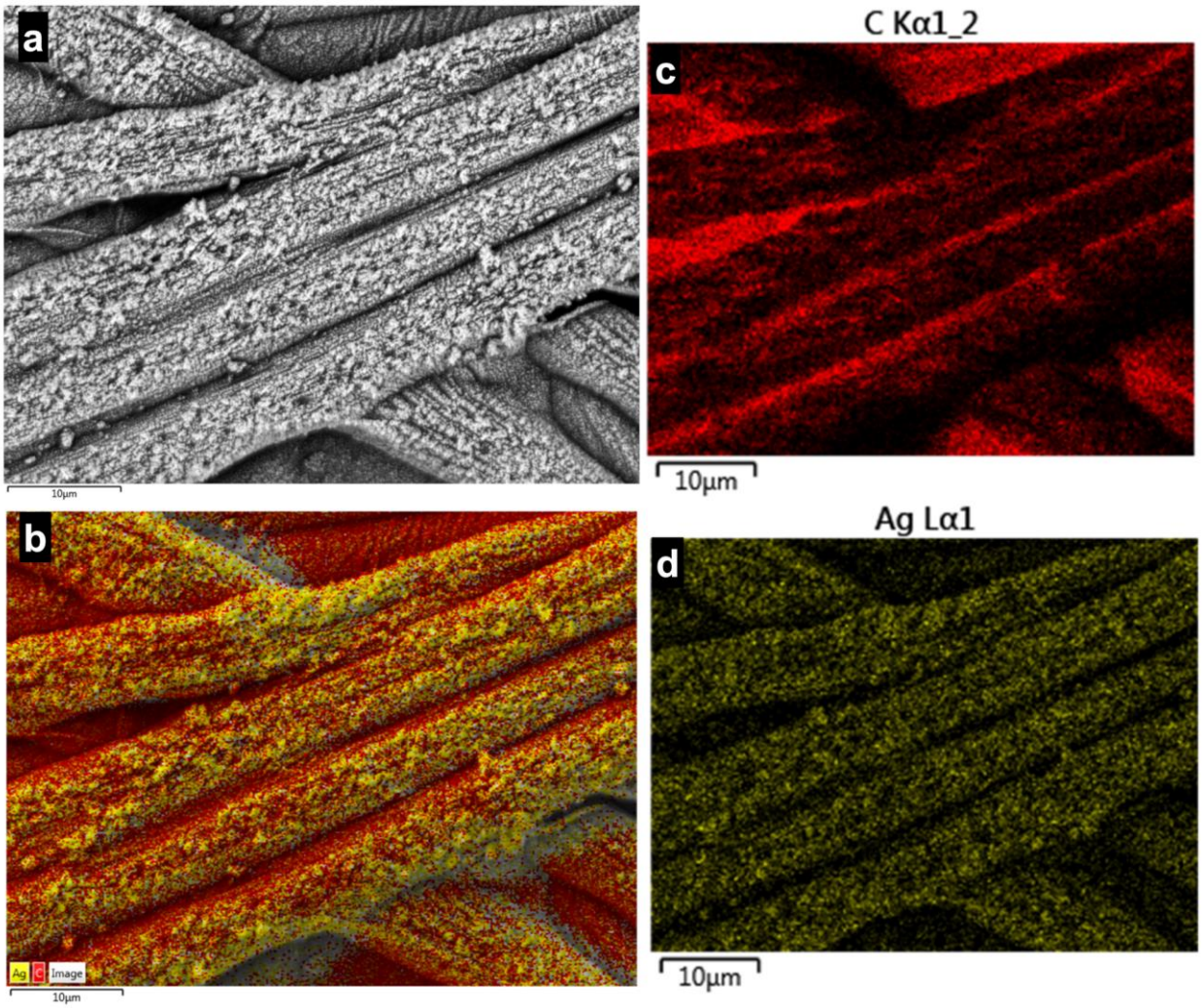

Fig. S8. EDX mapping of Ag grown onto a GDE for the ratio R = n(NH_4OH)/n($AgNO_3$) = 4 (a) SEM micrograph (during EDX) and the corresponding EDX elemental distribution maps of: (b) C+Ag, (c) C and (d) Ag. Synthesis conditions: 200 mM KNO_3, 0.30 mM $AgNO_3$, 1.20 mM NH_4OH, j_{appl} = -0.5 mA cm^{-2}; t_{OFF} = t_{ON} = 5 s; N_{cycles} = 252 and temperature = 25 °C

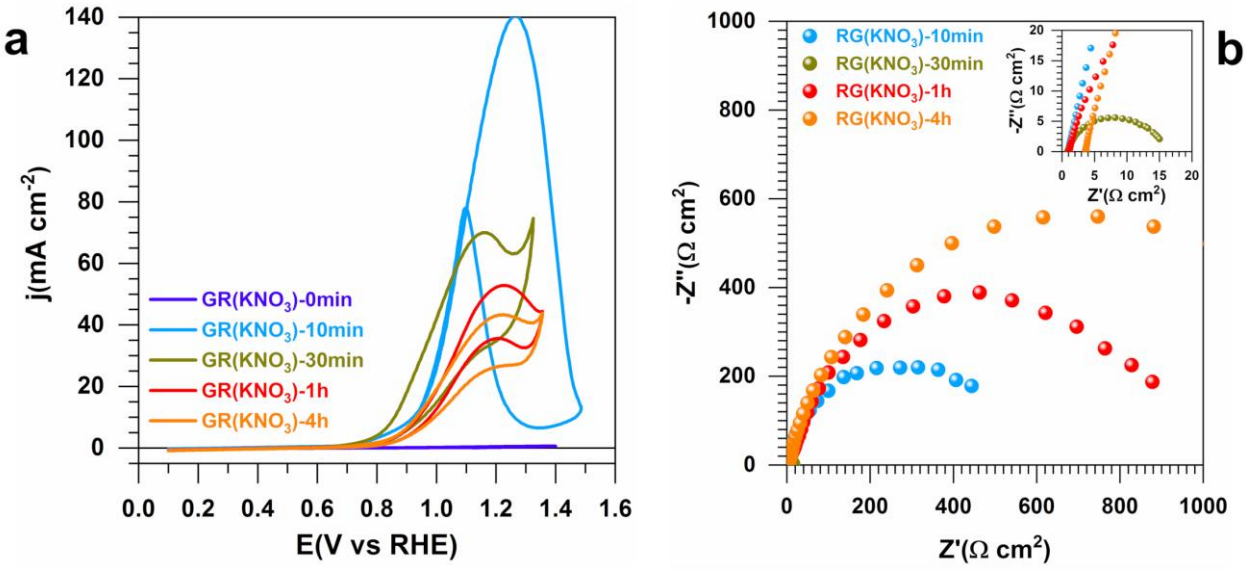

Fig. S9. Performance and characterization of the as-synthesized GDE@AgAu materials by the galvanic replacement (GR) performed in KNO_3.

(a) iR-free CVs recorded at 50 mV s^{-1} in 1 M KOH at 25 °C in presence of 0.1 M glycerol. (b) Complex-plane Nyquist impedance plots recorded at 0.9 V vs RHE in 1 M KOH + 0.1 glycerol at a temperature of 25 °C.

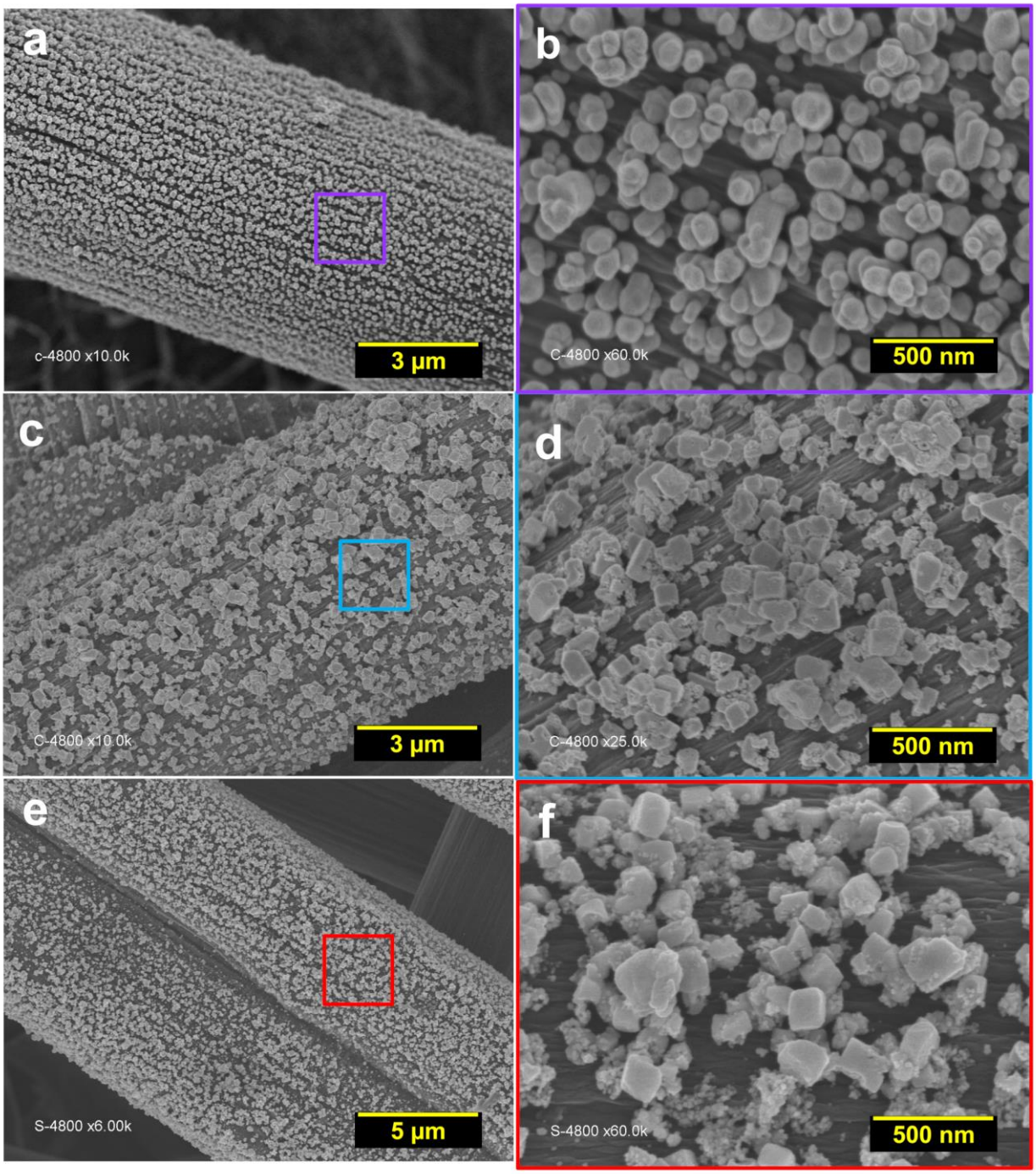

Fig. S10. Characterization of the as-synthesized GDE@AgAu materials for the galvanic replacement (GR) performed in KNO_3.

SEM/HRSEM micrographs for the reaction time: (a, b) 0, (c, d) 30 min, (e, f) 4 h.

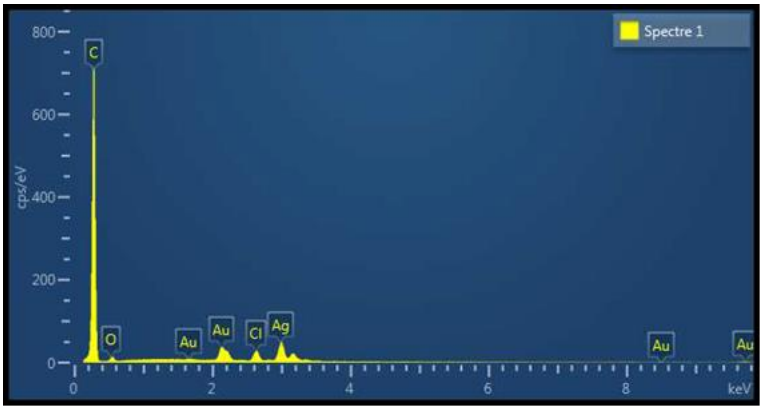

Fig. S11. EDX spectrum of the as-synthesized CP-AgAu-GR(KNO_3)-10min material. Pulse electrodeposition conditions: R = n(NH_4OH)/n($AgNO_3$) = 4, 200 mM KNO_3, 0.30 mM $AgNO_3$, j_{appl} = -0.5 mA cm^{-2}; t_{OFF} = t_{ON} = 5 s; N_{cycles} = 252 and temperature = 25 °C. Galvanic replacement (GR) conditions: 200 mM KNO_3, 487 μM $HAuCl_4$, t_{GR} = 10 min, temperature = RT, gentle shaking. Please: Read "Spectre" as "Spectrum".

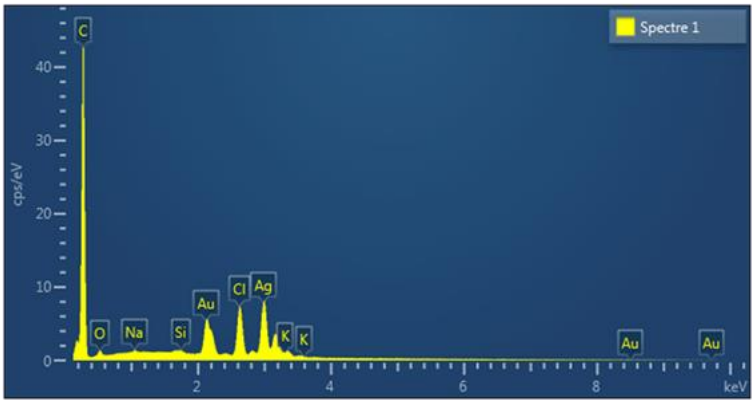

Fig. S12. EDX spectrum of the as-synthesized CP-AgAu-GR(KNO_3)-30min material. Pulse electrodeposition conditions: R = n(NH_4OH)/n($AgNO_3$) = 4, 200 mM KNO_3, 0.30 mM $AgNO_3$, j_{appl} = -0.5 mA cm^{-2}; t_{OFF} = t_{ON} = 5 s; N_{cycles} = 252 and temperature = 25 °C. Galvanic replacement (GR) conditions: 200 mM KNO_3, 487 µM $HAuCl_4$, t_{GR} = 30 min, temperature = RT, gentle shaking. Please: Read "Spectre" as "Spectrum".

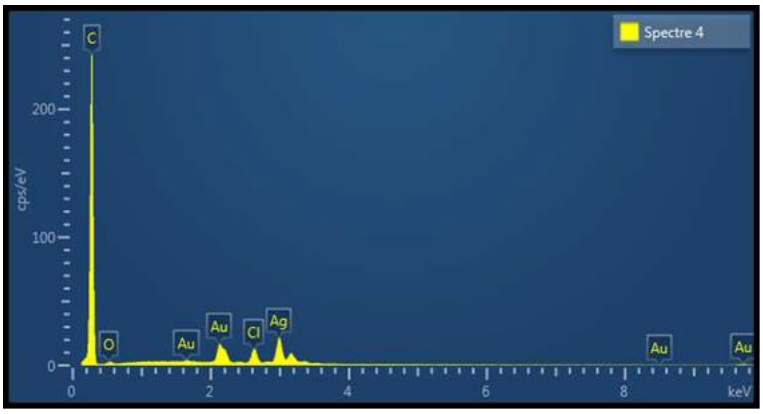

Fig. S13. EDX spectrum of the as-synthesized CP-AgAu-GR(H_2O)-10min material. Pulse electrodeposition conditions: R = n(NH_4OH)/n($AgNO_3$) = 4, 200 mM KNO_3, 0.30 mM $AgNO_3$, j_{appl} = -0.5 mA cm^{-2}; t_{OFF} = t_{ON} = 5 s; N_{cycles} = 252 and temperature = 25 °C. Galvanic replacement (GR) conditions: MQ water, 487 µM $HAuCl_4$, t_{GR} = 10 min, temperature = RT, gentle shaking. Please: Read "Spectre" as "Spectrum".

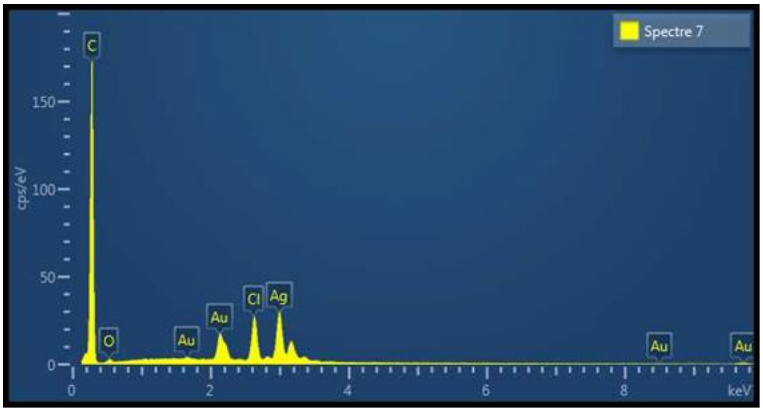

Fig. S14. EDX spectrum of the as-synthesized CP-AgAu-GR(H_2O)-5min material.
Pulse electrodeposition conditions: R = n(NH_4OH)/n($AgNO_3$) = 4, 200 mM KNO_3, 0.30 mM $AgNO_3$, j_{appl} = -0.5 mA cm^{-2}; t_{OFF} = t_{ON} = 5 s; N_{cycles} = 252 and temperature = 25 °C. Galvanic replacement (GR) conditions: MQ water, 487 μM $HAuCl_4$, t_{GR} = 5 min, temperature = RT, gentle shaking. Please: Read "Spectre" as "Spectrum".

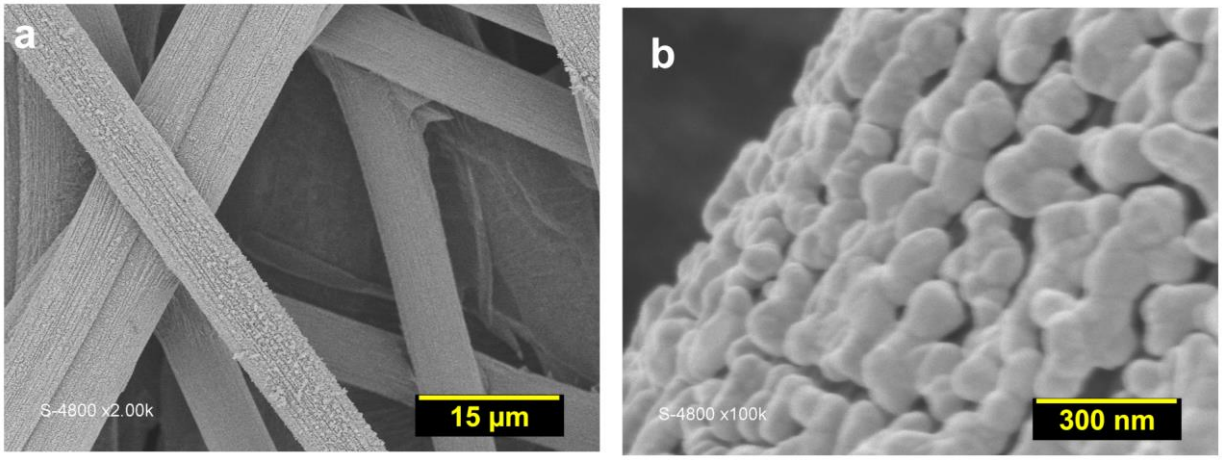

Fig. S15. SEM/HRSEM analysis of the as-synthesized GDL@Au materials referred to as "CP-Au".

(a) SEM and (b) HRSEM

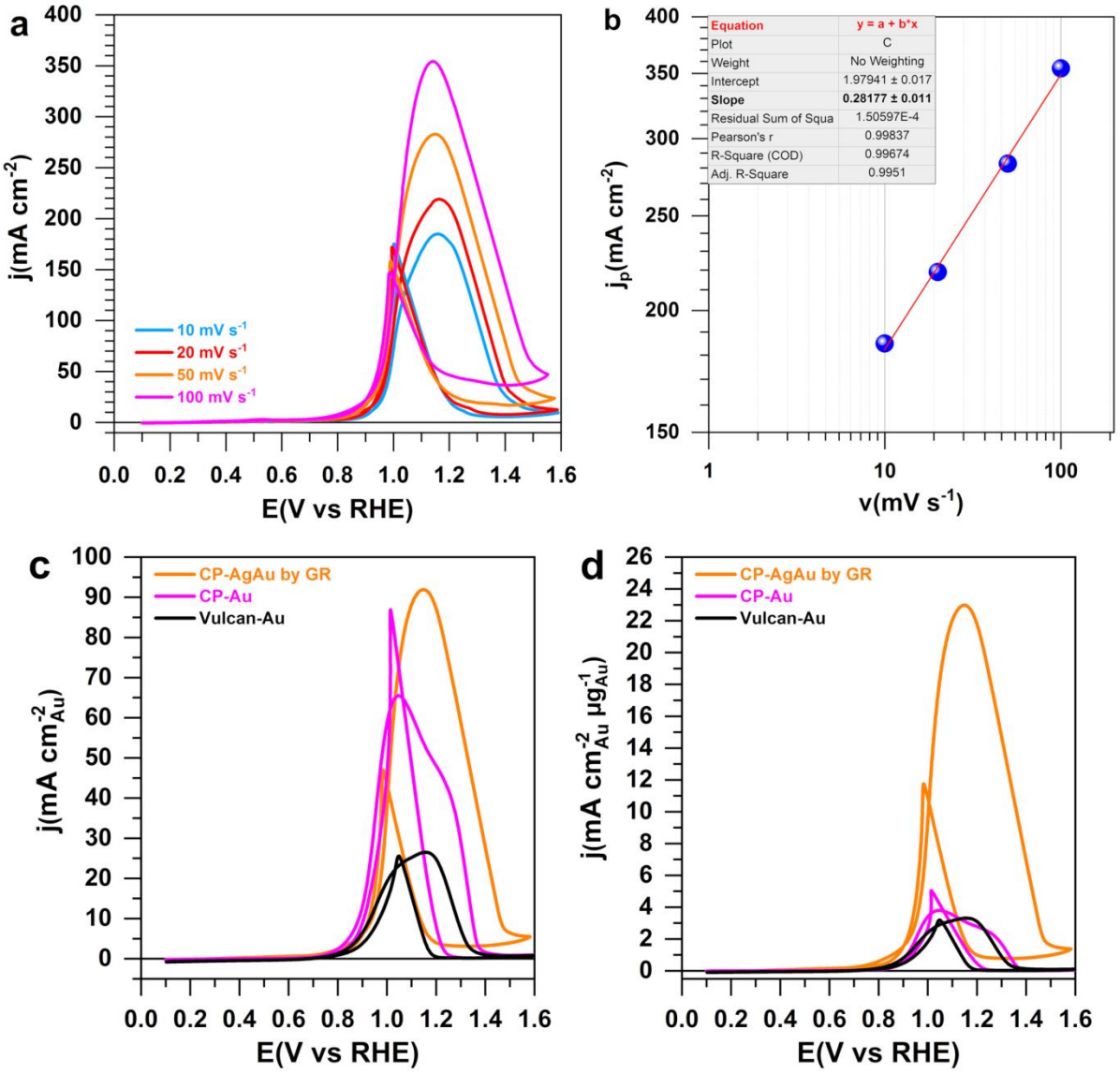

Fig. S16. Electrochemical characterization of the as-synthesized GD@AgAu material is the "CP-AgAu-GR(NaCl)-5min

(a) iR-free CVs in 1 M KOH + 0.1 glycerol at a temperature of 25 °C, and recorded at different scan rates. (b) Plot of "j_{peak}" vs "v" in log-log scale. (c) Normalized by the ECSA. (d) Normalized by both the ECSA and the Au weight.

Comments:

(1) The description of the CV of an organic molecule can be done by collecting CVs for different scan rates v = 1-200 mV s^{-1} and by plotting log(j_{peak}) vs log(v) where: (i) slope = 1 means that the reaction is limited by adsorption (reactants), (ii) slope = 0.5 means that the reaction is limited by diffusion (reactants and products), (iii) slope = 0.5-1 means that the reaction is limited by both adsorption and diffusion, and (iv) a slope < 0.5 is translated to as a

complex process (adsorption, diffusion, electron transfer). In the present case, the slope for the entire electrode materials is about 0.3, which falls in the last case. The result was expected since the glycerol electrooxidation reaction is a multi-proton and multi-electron transfer process so that the reactants diffusion, adsorption, products' diffusion and electrons transfer can simultaneously limit the overall reaction kinetic.

(2) the normalization of Figs. S17c-d is based on ECSA determined as following (in the blank electrolyte):

monolayer charge Q_0(μC cm^{-2})	482		
Scan rate (mV s^{-1})	50		
Electrode name	CP-Au	Vulcan-Au	CP-AgAu
electrode size (cm^2)	0.25	0.5	0.25
metal (Au)loading (μg cm^{-2})	69	16	16
Au(μg)	17.25	8	4
Oxide reduction peak area (mA V)	**0.00782408**	**0.020356**	**0.018921**
Q(μC)	156.5	407.1	378.4
ECSA(cm^2)	0.32	0.84	0.79
ECSA(m^2 g^{-1})	1.9	10.6	19.6

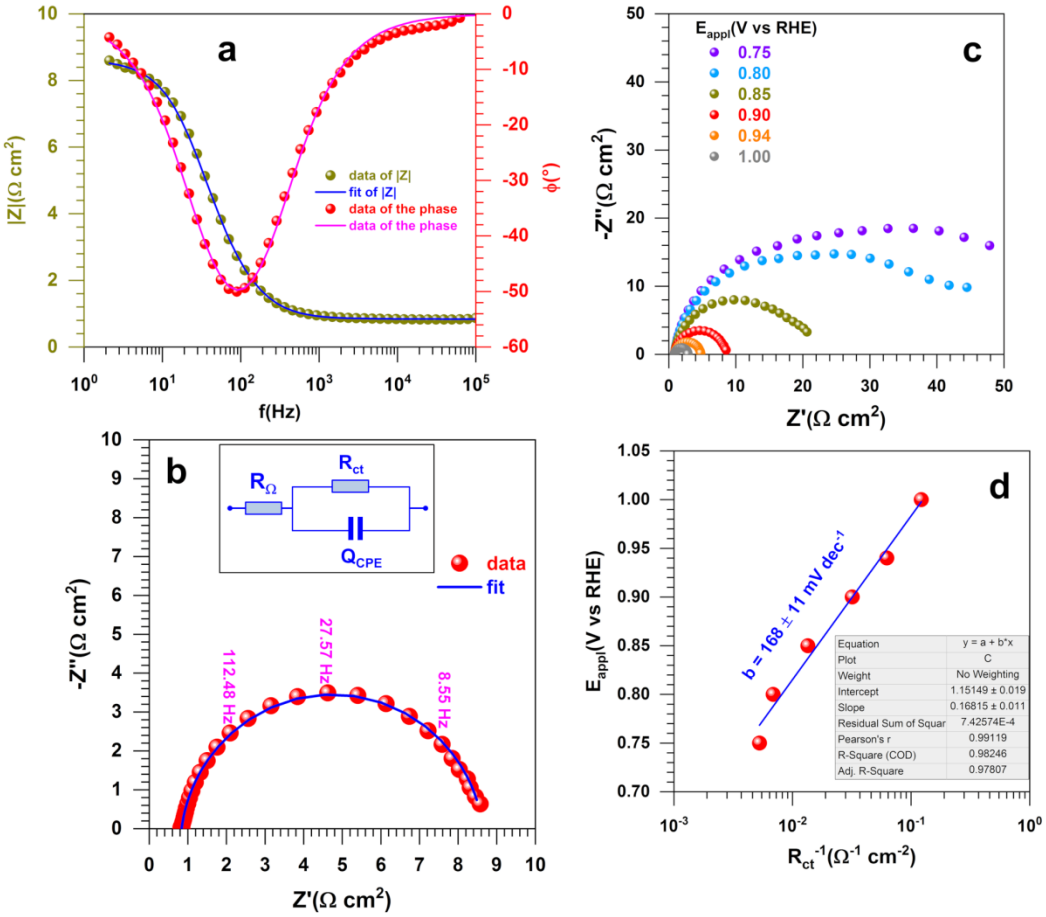

Figure S17. EIS characterization in 1 M KOH + 0.1 glycerol at 25 °C.

The as-synthesized GD@AgAu material is the "CP-AgAu-GR(NaCl)-5min". (a) Bode diagrams for E_{appl} = 0.9 V vs RHE. (b) Complex-plane Nyquist impedance plots for raw and fitted data (inset shows the used equivalent electrical circuit of R_{Ω}+Q_{CPE}//R_{ct} for fitting) for E_{appl} = 0.9 V vs RHE. (c) Nyquist impedance plots recorded at different electrode potentials. (d) Tafel plots by R_{ct}.

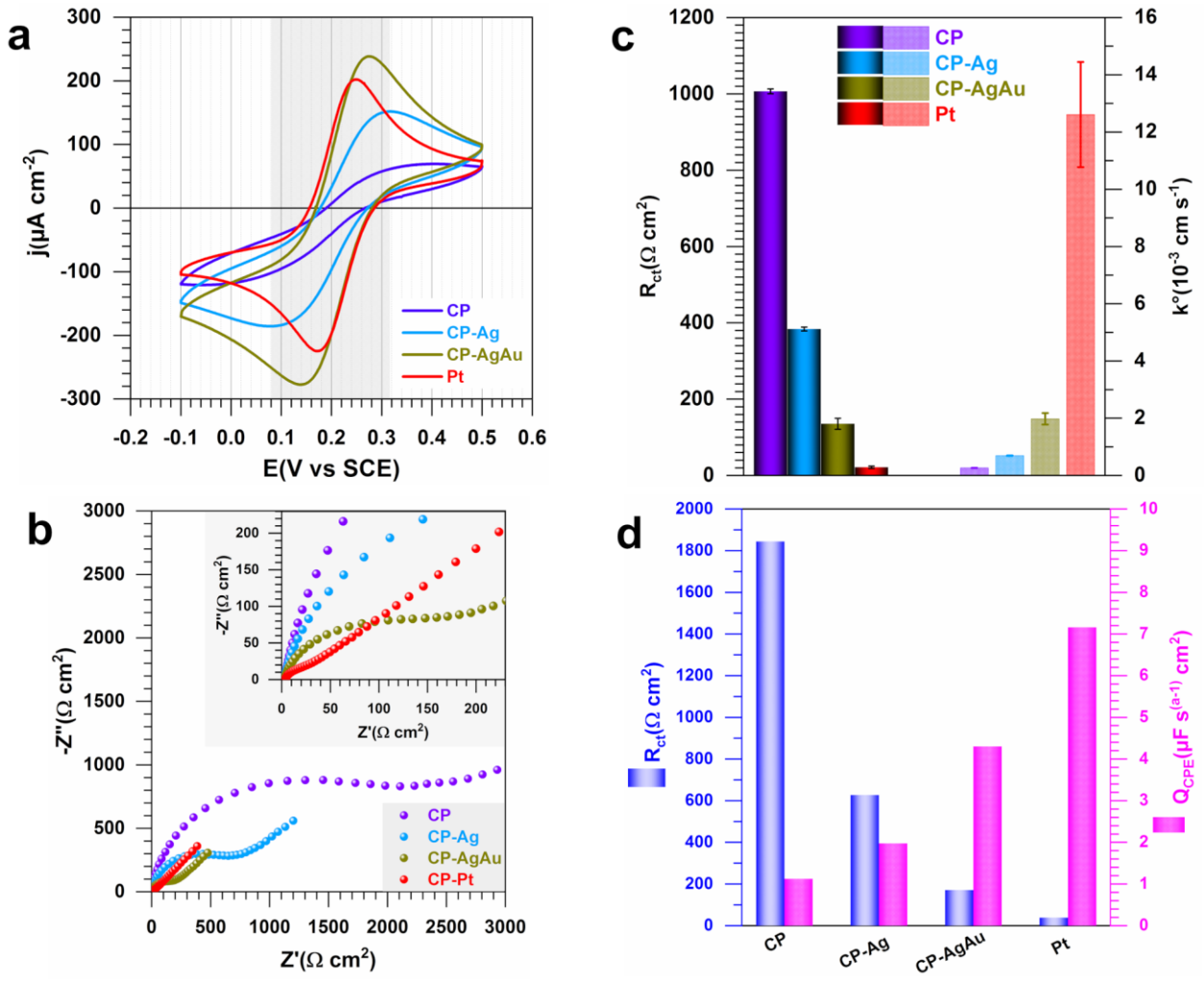

Fig. S18. Electrochemical characterization of the pristine CP, bulk Pt and the as-fabricated CP-Ag (GDE@Ag) and CP-AgAu (GDE@AuAg) materials in 0.5 M KNO_3 + 1 mM $K_3[Fe(CN)_6]$ at 25 °C.

(a) iR-free CVs recorded at 100 mV s^{-1}. (b) Complex-plane Nyquist impedance plots at E_{appl}(= OCP) = 0.25 ± 0.01 V vs SCE. (c) The values of R_{ct} (left *y*-axis) and k° (right y-axis) according to the method based on the peak-to-peak separation (ΔE_p) between the anodic and cathodic peaks on the CVs of panel (a) (see the detailed method in Figure S19): Error bars represent 1 SD (*n* = 3). (d) The value of R_{ct} (left *y*-axis) and Q_{CPE} (right *y*-axis) according to the EIS method using "R_Ω+Q_{CPE}//(R_{ct}+W)" as a representative equivalent electrical circuit to fit data from panel (b). For CP-AgAu, the galvanic replacement (GR) was performed in a brine solution.

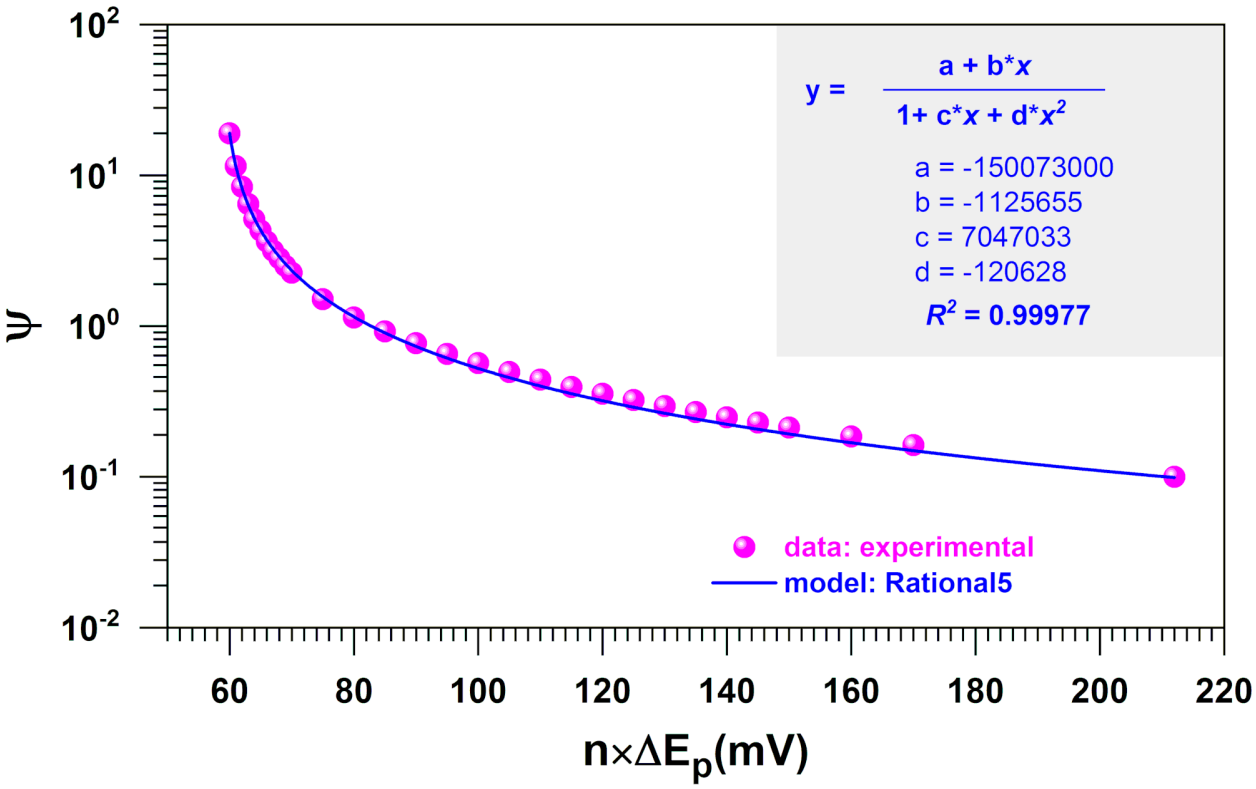

Fig. S19. Modeling curve of $n \times \Delta E_p$ vs. ψ (log-scale for ψ) for the determination of the kinetics data from the analysis of the peak separation, ΔE_p between the anodic and cathodic peaks on a CV.

Experimental data were taken from refs.[22,23] Specifically, standard rate constant (k°), charge transfer resistance (R_{ct}) and exchange current density (j_0) were extracted from the relations explicated below.[22-28] Since α is mostly in the range of 0.4-0.6 and D_{Ox} is closer to D_{Red}, hence, one can assume that $\gamma^{\alpha} \approx 1$.

$$k^{\circ} = \frac{\psi}{\left(\frac{D_{Ox}}{D_{Red}}\right)^{\alpha} \sqrt{\frac{RT}{\pi n v F D_{Ox}}}} \qquad \gamma = \frac{D_{Ox}}{D_{Red}}$$

$$R_{ct} = \left[\frac{RT}{(nF)^2 C}\right]\frac{1}{k^{\circ}} \qquad j_0 = \left[\frac{RT}{nF}\right]\frac{1}{R_{ct}} = [nFC]k^{\circ}$$

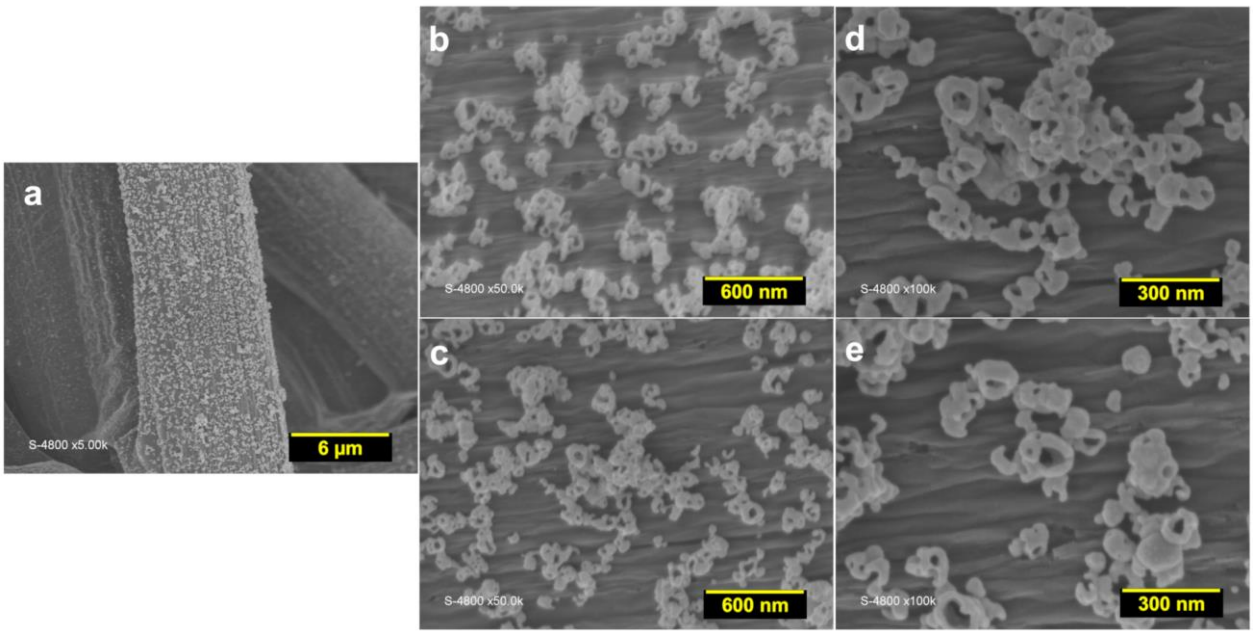

Fig. S20. SEM/HRSEM micrographs for the as-synthesized GDE@AgAu materials by the galvanic replacement (GR) performed in H_2O (5 min) and subsequently washed with a brine solution, referred to as GR(H_2O)-washed(NaCl)

(a-e) SEM/HRSEM micrographs at different magnifications

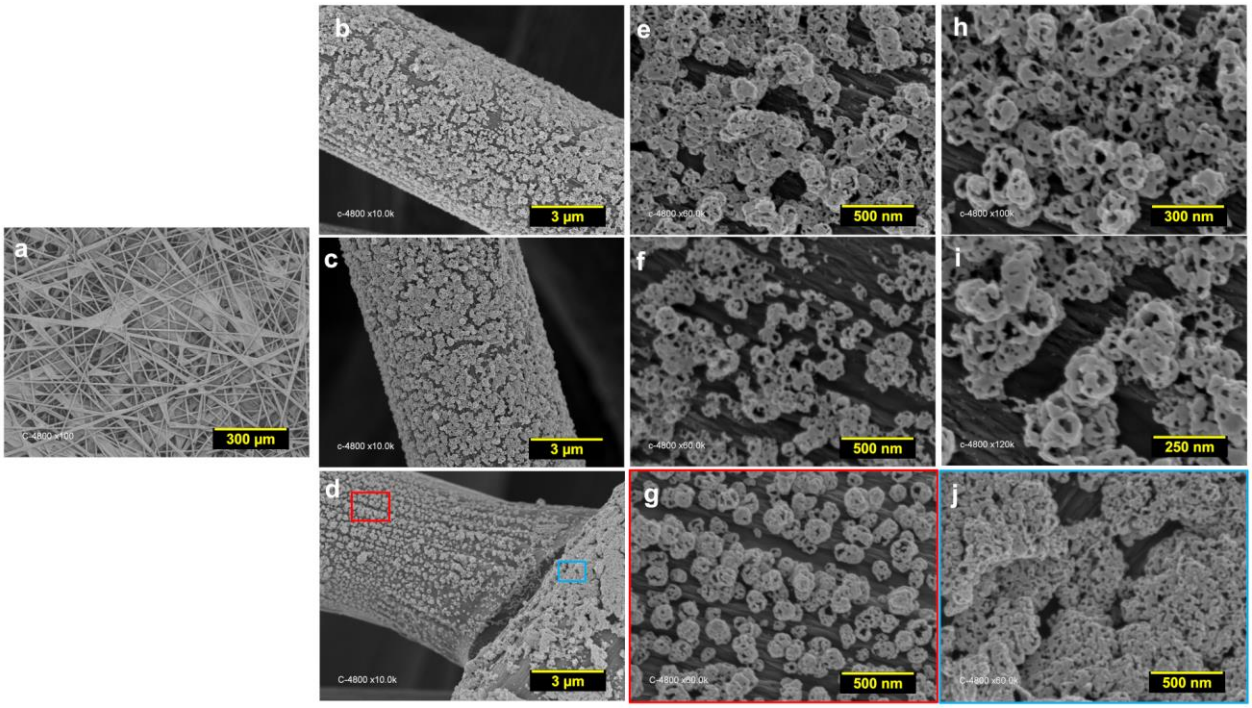

Fig. S21. SEM/HRSEM micrographs for the as-synthesized GDE@AgAu materials by the galvanic replacement (GR) performed in a brine solution (5 min), referred to as GR(NaCl). (a-j) SEM/HRSEM micrographs at different magnifications.

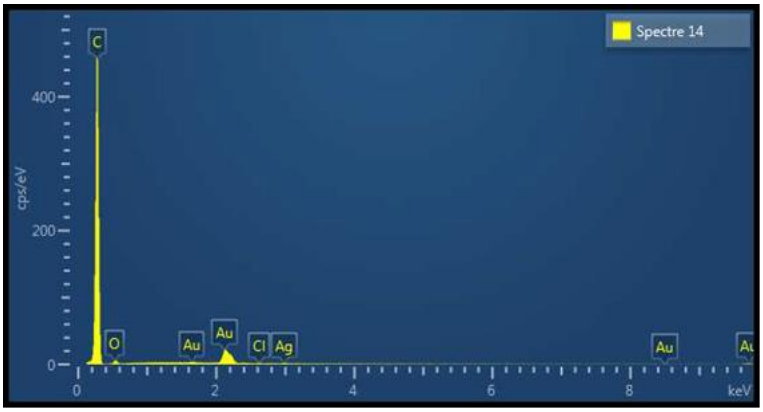

Fig. S22. EDX spectrum of the as-synthesized CP-AgAu-GR(H_2O)-washed(NaCl)-5min material.

Pulse electrodeposition conditions: R = n(NH_4OH)/n($AgNO_3$) = 4, 200 mM KNO_3, 0.30 mM $AgNO_3$, j_{appl} = -0.5 mA cm^{-2}; t_{OFF} = t_{ON} = 5 s; N_{cycles} = 252 and temperature = 25 °C. GR conditions: MQ water, 487 µM $HAuCl_4$, t_{GR} = 5 min, temperature = RT, gentle shaking. Please: Read "Spectre" as "Spectrum".

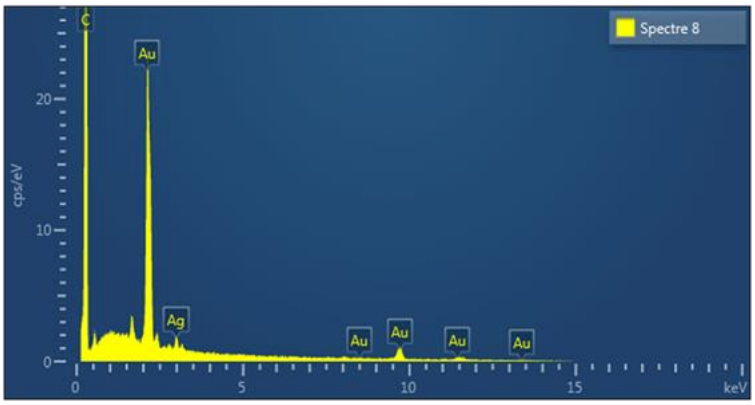

Fig. S23. EDX spectrum of the as-synthesized CP-AgAu-GR(NaCl)-5min material.

Pulse electrodeposition conditions: R = n(NH_4OH)/n($AgNO_3$) = 4, 200 mM KNO_3, 0.30 mM $AgNO_3$, j_{appl} = -0.5 mA cm^{-2}; t_{OFF} = t_{ON} = 5 s; N_{cycles} = 252 and temperature = 25 °C. GR conditions: MQ water, 487 µM $HAuCl_4$, t_{GR} = 5 min, temperature = RT, gentle shaking. Please: Read "Spectre" as "Spectrum".

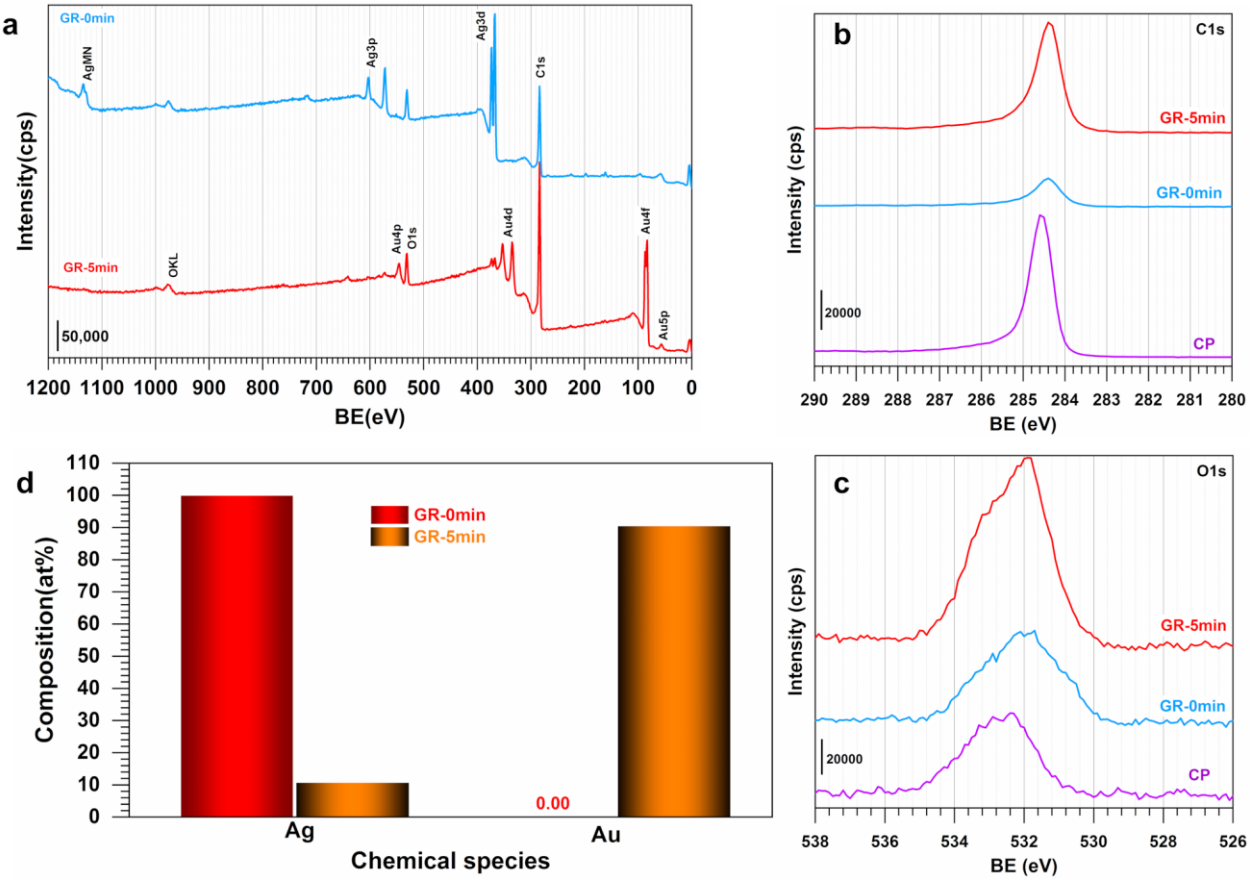

Fig. S24. XPS characterization of the as-prepared materials.

CP referred to as the GDE; GR-0 referred to as GDE@Ag, GR-5min referred to as GDE@AgAu obtained by the galvanic replacement (GR) performed in a brine solution, CP-Au is the control synthesis of monometallic. (a) Survey XPS spectra. (b) High-resolution XPS spectra of the C 1s core level. (c) High-resolution XPS spectra of the O 1s core level. (d) Quantitative data.

The absence of oxide peaks from XPS of Au 4f and Ag 3d endorses completely the conclusion that the majority of the observed oxygen is simply due to the starting materials of CP, which has been characterized by XPS elsewhere.[2]

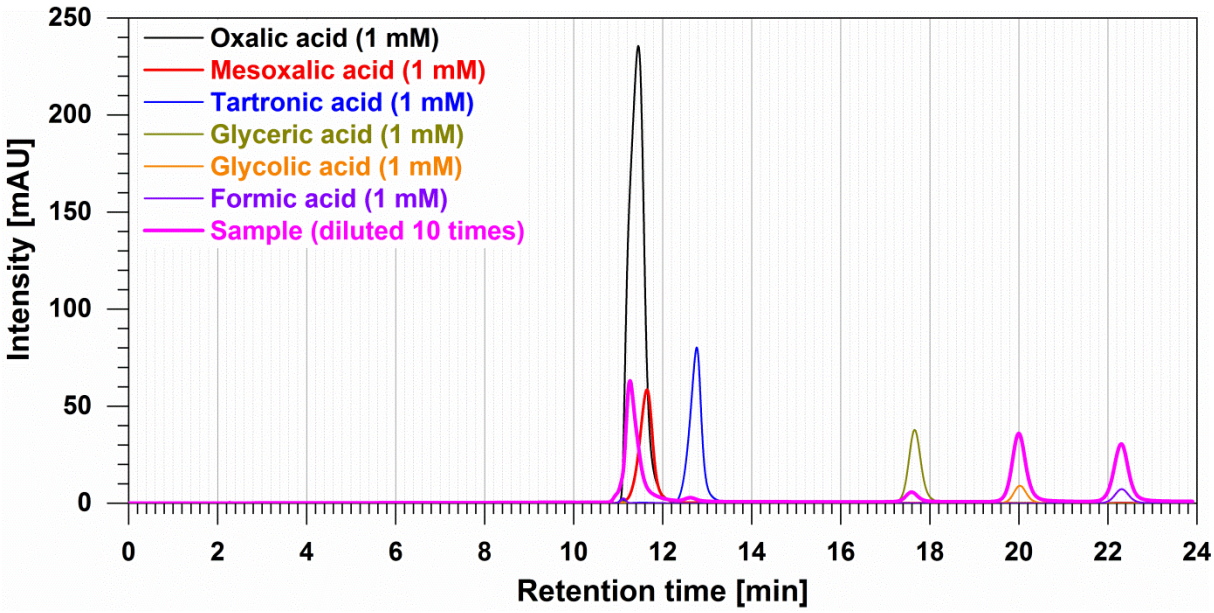

Fig. S25. Overview of the chromatograms obtained from HPLC analysis.

Eluent: 3 mM H2SO4; injection: 25 µL; column BP-OA Benson 2000-0, 30 cm, at room temperature. External compounds at 1 mM and the sample (diluted 10 times) from the electrolysis at GDE@AgAu catalyst material obtained by GR in a brine solution.

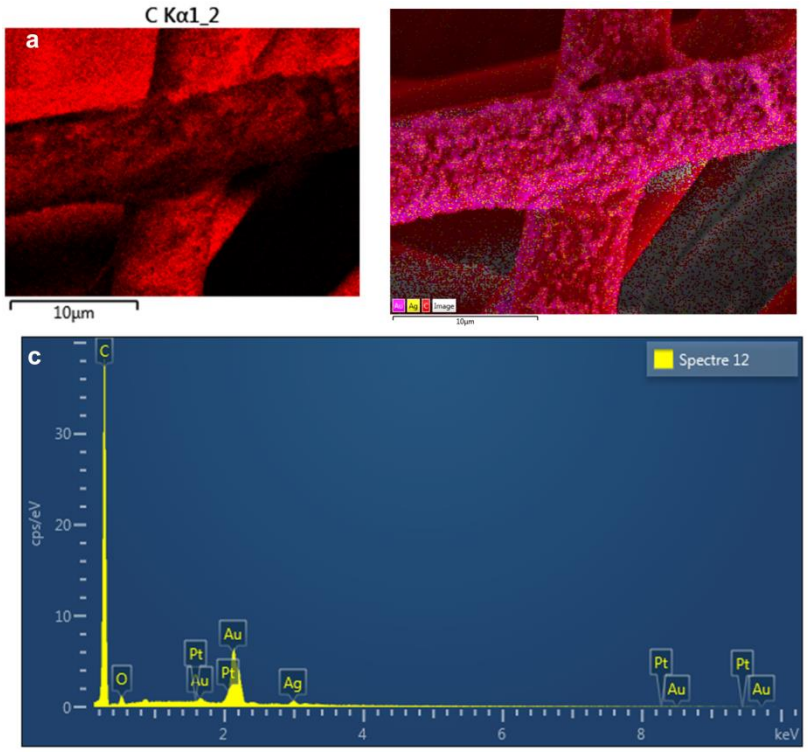

Fig. S26. Post-mortem SEM and EDX of the as-synthesized CP-AgAu-GR(NaCl)-5min material after 3 h of bulk electrolysis.

$E_{applied}$ = 0.3 V vs MOE = 1.246 V vs RHE with no iR-drop correction. Temperature = 25 °C. (a) EDX mapping of C. (b) EDX mapping of C+Ag+Au. (c) EDX spectrum. NB: Signal of Pt comes from the sample preparation to enhance the SEM/HRSEM imaging capability. Please: Read “Spectre” as “Spectrum”.

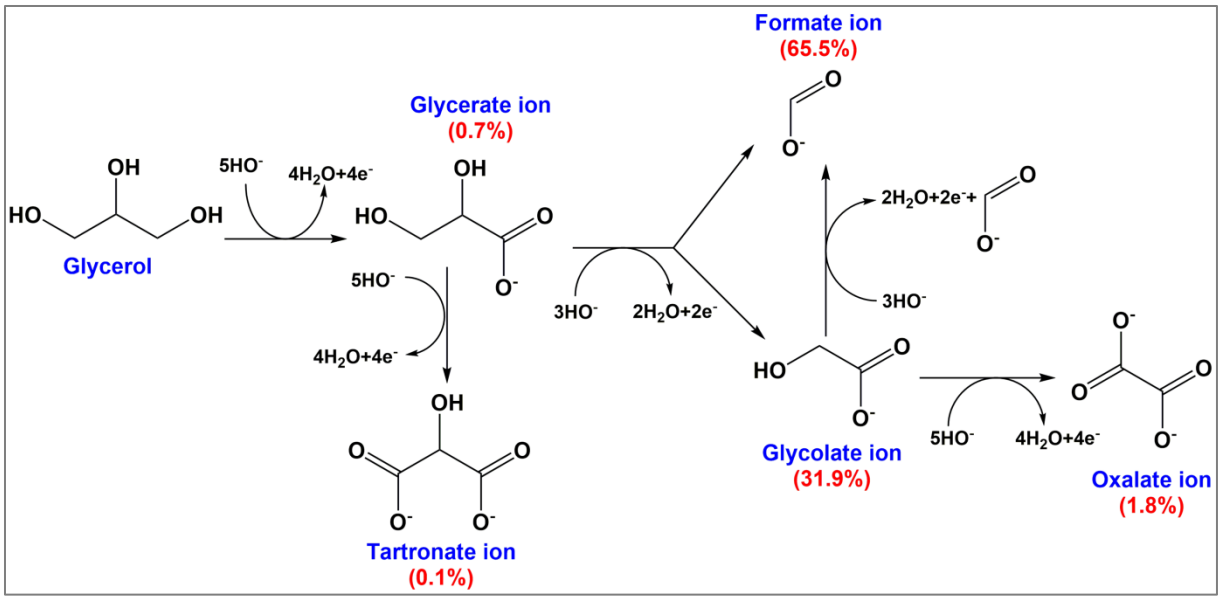

Scheme S1. Proposed reaction scheme for glycerol electrooxidation in alkaline medium on the as-synthesized silver-gold nanoporous and nanoalloyed nanocatalysts.

Numbers in red and in brackets indicate that the reaction product selectivity quantified by HPLC.

References

1. Y. Holade, R. G. da Silva, K. Servat, T. W. Napporn, C. Canaff, A. R. De Andrade and K. B. Kokoh, *J. Mater. Chem. A*, 2016, **4**, 8337-8349.
2. M. Weber, N. Tuleushova, J. Zgheib, C. Lamboux, I. Iatsunskyi, E. Coy, V. Flaud, S. Tingry, D. Cornu, P. Miele, M. Bechelany and Y. Holade, *Appl. Catal. B: Env.*, 2019, **257**, 117917.
3. Y. Holade, C. Morais, K. Servat, T. W. Napporn and K. B. Kokoh, *ACS Catal.*, 2013, **3**, 2403-2411.
4. V. L. Oliveira, C. Morais, K. Servat, T. W. Napporn, G. Tremiliosi-Filho and K. B. Kokoh, *Electrochim. Acta*, 2014, **117**, 255-262.
5. V. L. Oliveira, C. Morais, K. Servat, T. W. Napporn, G. Tremiliosi-Filho and K. B. Kokoh, *J. Electroanal. Chem.*, 2013, **703**, 56-62.
6. Y. Kwon, K. J. P. Schouten and M. T. M. Koper, *ChemCatChem*, 2011, **3**, 1176-1185.
7. Z. Chen, C. Liu, X. Zhao, H. Yan, J. Li, P. Lyu, Y. Du, S. Xi, K. Chi, X. Chi, H. Xu, X. Li, W. Fu, K. Leng, S. J. Pennycook, S. Wang and K. P. Loh, *Adv. Mater.*, 2019, **31**, 1804763.
8. S. Li, J. Lai, R. Luque and G. Xu, *Energy Environ. Sci.*, 2016, **9**, 3097-3102.
9. W. Hong, C. Shang, J. Wang and E. Wang, *Energy Environ. Sci.*, 2015, **8**, 2910-2915.
10. Y. Zhou, Y. Shen and J. Xi, *Appl. Catal. B: Env.*, 2019, **245**, 604-612.
11. Y. Zhou, Y. Shen, J. Xi and X. Luo, *ACS Appl. Mater. Interfaces.*, 2019, **11**, 28953-28959.
12. H. Xu, J. Wei, M. Zhang, C. Wang, Y. Shiraishi, J. Guo and Y. Du, *J. Mater. Chem. A*, 2018, **6**, 24418-24424.
13. H. Xu, J. Wang, B. Yan, K. Zhang, S. Li, C. Wang, Y. Shiraishi, Y. Du and P. Yang, *Nanoscale*, 2017, **9**, 12996-13003.
14. A. Zalineeva, A. Serov, M. Padilla, U. Martinez, K. Artyushkova, S. Baranton, C. Coutanceau and P. B. Atanassov, *J. Am. Chem. Soc.*, 2014, **136**, 3937-3945.
15. L. M. Palma, T. S. Almeida, V. L. Oliveira, G. Tremiliosi-Filho, E. R. Gonzalez, A. R. de Andrade, K. Servat, C. Morais, T. W. Napporn and K. B. Kokoh, *RSC Adv.*, 2014, **4**, 64476-64483.
16. M. Simões, S. Baranton and C. Coutanceau, *Appl. Catal. B: Env.*, 2010, **93**, 354-362.

17. J. González-Cobos, S. Baranton and C. Coutanceau, *ChemElectroChem*, 2016, **3**, 1694-1704.
18. L. M. Palma, T. S. Almeida, C. Morais, T. W. Napporn, K. B. Kokoh and A. R. de Andrade, *ChemElectroChem*, 2017, **4**, 39-45.
19. A. Serov, U. Martinez and P. Atanassov, *Electrochem. Commun.*, 2013, **34**, 185-188.
20. D. Xu, Y. Liu, S. Zhao, Y. Lu, M. Han and J. Bao, *Chem. Commun.*, 2017, **53**, 1642-1645.
21. M. Weber, P. Collot, H. El Gaddari, S. Tingry, M. Bechelany and Y. Holade, *ChemElectroChem*, 2018, **5**, 743-747.
22. R. S. Nicholson, *Anal. Chem.*, 1965, **37**, 1351-1355.
23. J. Heinze, *Angew. Chem. Int. Ed.*, 1984, **23**, 831-847.
24. A. J. Bard and L. R. Faulkner, *Electrochemical Methods: Fundamentals and Applications*, John Wiley & Sons, Inc., USA, 2nd edn., 2001.
25. A. J. Bard and L. R. Faulkner, *Electrochemical Methods: Fundamentals and Applications*, John Wiley & Sons, Inc., USA, 1st edn., 1980.
26. E. Mahé, D. Devilliers and C. Comninellis, *Electrochim. Acta*, 2005, **50**, 2263-2277.
27. A. L. Eckermann, D. J. Feld, J. A. Shaw and T. J. Meade, *Coord. Chem. Rev.*, 2010, **254**, 1769-1802.
28. D. Salinas-Torres, F. Huerta, F. Montilla and E. Morallón, *Electrochim. Acta*, 2011, **56**, 2464-2470.